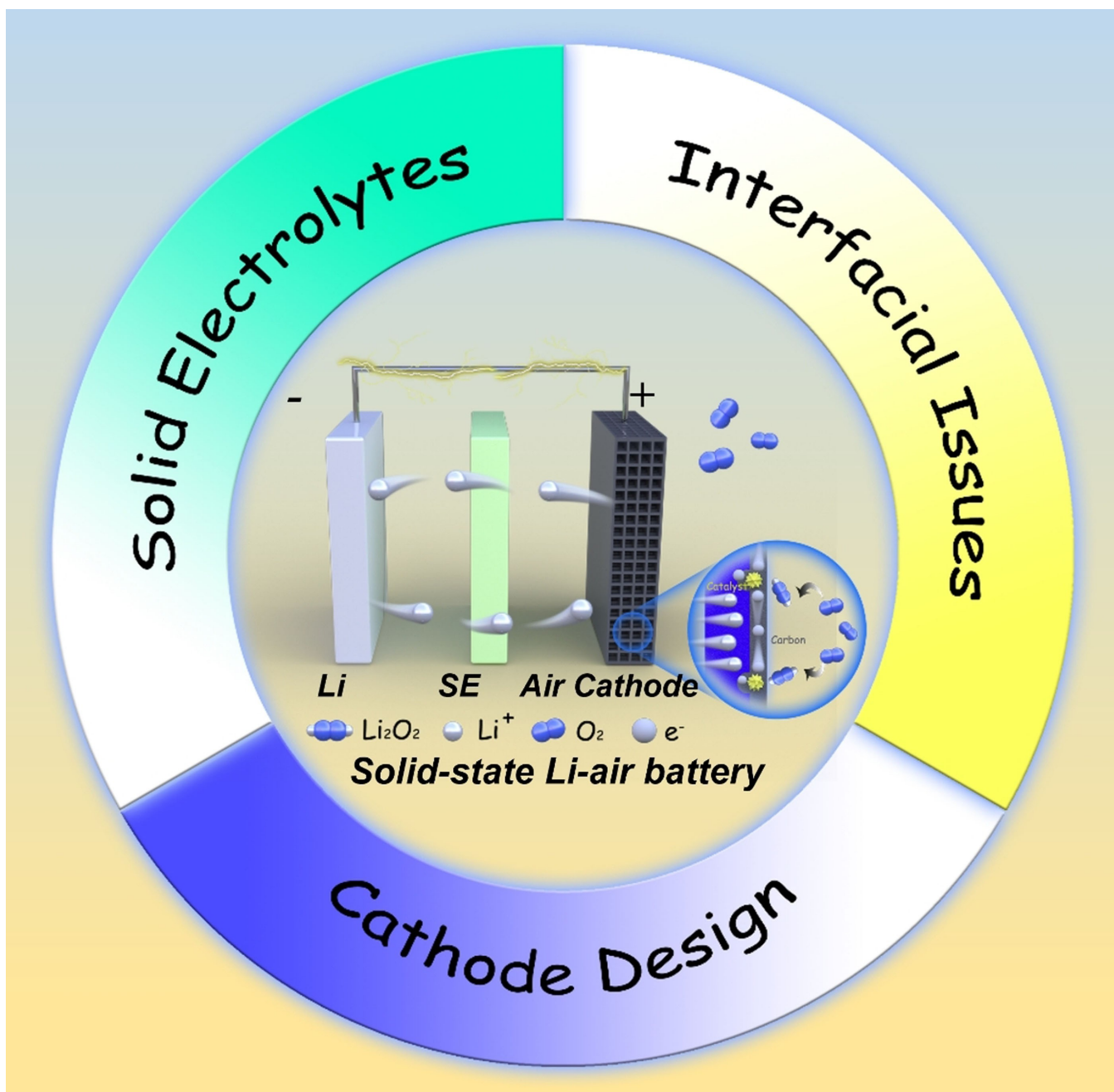


Advancements, Challenges, and Prospects in Rechargeable Solid-State Lithium-Air Batteries

Zhi Gu,^[a, c] Xing Xin,^[d] Mingyang Men,^[a, b] Yangyang Zhou,^[a, b] Jinghua Wu,^[a, b] Yong Sun,^{*[c, e]} and Xiayin Yao^{*[a, b]}



Solid-state lithium-air batteries (SSLABs) are attracting widespread research interest as emerging energy storage systems with ultra-high theoretical energy density. However, due to their relatively short development history, the practical capacity and cyclic performance of SSLABs still fail to meet application requirements. The selection of solid electrolytes and the design and optimization of air cathodes are key factors for developing high-performance solid-state lithium-air batteries. In this review, we focus on recent scientific advances and challenges in SSLABs, providing a comprehensive overview of solid electro-

lytes, air cathodes, and interface issues. Strategies such as electrolyte modification, composite cathodes, interface engineering, and the addition of catalysts which have been effective in addressing issues related to low ionic conductivity of electrolytes, high interfacial impedance, sluggish kinetics of electrochemical reactions, and poor cycling stability, were reviewed and discussed. Furthermore, this review also discusses the prospects of SSLABs, aiming to inspire and provide references for the development of solid-state lithium-air batteries, as well as other metal-air batteries.

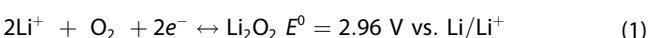
1. Introduction

The widespread adoption of new energy technologies has driven the rapid development of electric vehicles (EVs) and portable electronic devices (PEDs). However, the current lithium-ion and lithium metal battery systems fall short in meeting the ever-growing demand for larger battery energy density. As a consequence, emerging high-energy battery technologies are being explored as potential alternatives to conventional lithium-ion batteries. One such system is the lithium-air (Li-air) or lithium-oxygen (Li–O₂) battery, which has attracted significant attention due to its exceptionally high theoretical energy density of 3,500 Wh kg⁻¹. The concept of Li-air batteries was initially introduced in the 1970s by Littauer and Tsai et al.^[1] and a subsequent breakthrough in rechargeable Li-air batteries in 1996 triggered a surge of research in this field.^[2] Consequently, extensive investigations have been undertaken to elucidate the electrode reaction mechanism, optimize the electrolyte, explore novel electrode materials, and improve other structural components of Li-air batteries.^[3]

Li-air batteries belong to the category of metal-air batteries (MABs), which typically comprise a metal anode, an electrolyte, and an air electrode. MABs utilize the air as an active material during the electrochemical reaction involved in the battery. This distinctive characteristic confers metal-air batteries with exceptionally high theoretical specific energy (exceeding 1000 Wh kg⁻¹), which excludes the mass of oxygen. Albeit many

types of MABs candidates, such as zinc-air, magnesium-air, and aluminum-air batteries have been extensively investigated and the zinc-air batteries even reach the phase of commercialization, the Li-air batteries still attract enduring and massive interests both from industrial and academia. This lies in the remarkable intrinsic features of lithium: a) lithium possesses the lowest redox potential (-3.03 V vs. the standard hydrogen electrode, SHE), b) it has the smallest electrochemical equivalent (0.259 g Ah⁻¹) among all other metallic elements.

The reaction mechanism of conventional non-aqueous Li-air batteries involves oxygen (O₂) participating in both the charging and discharging processes. The dominant overall reaction can be represented as follows:



During discharge, as the battery supplies power, oxygen molecules at the cathode are reduced, forming lithium peroxide (Li₂O₂). Simultaneously, lithium metal at the anode undergoes oxidation, releasing lithium ions. The electrolyte contains lithium salts that provide a source of soluble lithium ions. Conversely, during the charge process, the discharge product Li₂O₂ decomposes into Li and O₂. At the same time, lithium ions migrate back to the anode, where they are reduced back to metallic lithium. It is worth noting that the efficient functioning of Li-air batteries relies on good oxygen permeability and a large electrode surface area for effective reactions with oxygen from the surrounding air. This property contributes to the high theoretical energy density, making Li-air batteries an attractive option for high-energy-density applications. However, challenges related to oxygen supply, side reactions, and electrode stability need to be addressed before these batteries can be widely implemented.

According to the fundamental research on the Li-air batteries,^[2,4] it has been determined that critical elements for improving their performance include the careful adjustment of electrolyte composition, the advancement of novel electrode materials, and the successful regulation of undesired byproduct formation. These efforts essentially enhance the efficiency and stability of Li-air batteries. Regarding electrolyte selections, most Li-air batteries utilize aprotic or aqueous liquid electrolytes,^[5] which inevitably encounters the thorny problems, i.e., capacity decay, rapid degradation of cycling performance, safety hazards due to potential leaks, and formation of passivation layers impeding the diffusion of oxygen. Adopting

- [a] Dr. Z. Gu, M. Men, Y. Zhou, Prof. J. Wu, Prof. X. Yao
Ningbo Institute of Materials Technology and Engineering, Chinese Academy of Sciences, Ningbo 315201, P. R. China
E-mail: yaoxy@nimte.ac.cn
Homepage: <https://yaoxy.nimte.ac.cn>
- [b] M. Men, Y. Zhou, Prof. J. Wu, Prof. X. Yao
Center of Materials Science and Optoelectronics Engineering, University of Chinese Academy of Sciences, Beijing 100049, P. R. China
- [c] Dr. Z. Gu, Prof. Y. Sun
Department of Chemical and Environmental Engineering, Faculty of Science and Engineering, University of Nottingham, Ningbo, 315100, China
E-mail: y.sun@ecu.edu.au
Homepage: <https://research.nottingham.edu.cn/en/persons/yong-sun>
- [d] Prof. X. Xin
School of Material Science and Chemical Engineering, Ningbo University, Ningbo 315211, P. R. China
- [e] Prof. Y. Sun
School of Engineering, Edith Cowan University, 270 Joondalup Drive Joondalup WA 6027 Australia

solid electrolytes offers a valuable solution to tackle aforementioned challenges and enhance the practicability of Li-air batteries. While the exact definition of a solid-state Li-air battery may vary, it generally entails an electrolyte layer formed by a non-liquid material, such as glass-ceramic or polymer. Quasi-solid Li-air batteries, which use a liquid electrolyte to wet the electrolyte-electrode interface or employ a solid-liquid hybrid or gel electrolyte, are considered as a compromising solution. The composition of a typical solid-state Li-air battery consists of a lithium metal, a solid electrolyte, and a carbon-based air cathode. A solid-state lithium-air battery operates by enabling the migration of lithium ions from the anode to the cathode through a solid-state electrolyte, while simultaneously facilitat-

ing the reduction of oxygen molecules at the cathode. The oxygen reduction reaction at the cathode leads to the formation of oxide ions, which travel through the electrolyte. At the cathode, these oxide ions combine with the migrating lithium ions to form either lithium oxide or lithium peroxide, depending on the specific battery design. The operating mechanism of solid-state Li-air batteries remains a subject of debate. Some researchers have proposed that these batteries follow a mechanism similar to non-aqueous liquid systems, involving the formation and decomposition of Li_2O_2 . However, this mechanism has not been extensively studied due to the lack of a suitable solid-state electrolyte and coordinated cathode. During the discharge process, Li_2O is formed, followed



Zhi Gu received his BEng in Environmental Engineering from University of Nottingham in 2017 and achieved his MSc in Environmental Systems Engineering in University College London. He is currently pursuing his Ph.D. degree under the supervision of Professor Xiayin Yao and Dr. Yong Sun at Ningbo Institute of Materials Technology and Engineering, Chinese Academy of Sciences (NIMTE, CAS) and University of Nottingham Ningbo China (UNNC). His research work focuses on rational design and performance study of solid-state lithium-air or lithium-oxygen batteries.



Xing Xin is an associate professor at Ningbo University. She received her Bachelor of Science (BS) degree from Shandong University, China in 2006 and her Ph.D. degree from Ningbo Institute of Materials Technology and Engineering, Chinese Academy of Sciences in 2013. After postdoctoral research at the National Institute for Materials Science (NIMS, Japan), She joined Ningbo University as an associate professor in 2018. Her research interests focus on electrochemical catalysis and lithium-air batteries.



Mingyang Men is a postgraduate student at Ningbo Institute of Materials Technology and Engineering, Chinese Academy of Sciences. His research interests focus on the development of solid state lithium batteries.



Yangyang Zhou is pursuing his Ph.D. at Ningbo Institute of Materials Technology and Engineering, Chinese Academy of Sciences. His research interest is solid state lithium batteries.



Jinghua Wu is a professor at Ningbo Institute of Materials Technology and Engineering, Chinese Academy of Science (NIMTE, CAS). He received his Bachelor of Science (BS) degree from Shandong University, China in 2006 and his Ph.D. degree from NIMTE in 2012. After postdoctoral research at the National Institute for Materials Science (NIMS, Japan) and Soochow University, he joined NIMTE in 2018. His research interests focus on sulfide-electrolyte-based solid-state batteries.



Yong Sun received his Ph.D. in Chemical Engineering from Institute of Process of Engineering, Chinese Academy of Sciences (IPE, CAS) in 2008. He is currently working as Associate Professor at University of Nottingham Ningbo China (UNNC) and Associate Professor adjunct at School of Engineering, Edith Cowan University (Australia). His research focuses on lithium battery recycling, phase diagram, reaction kinetics through supervised machine learning approach.



Xiayin Yao is a professor at Ningbo Institute of Materials Technology and Engineering, Chinese Academy of Sciences (NIMTE, CAS). He received his Ph.D. from Institute of Solid State Physics and NIMTE, CAS in 2009. After that, he joined NIMTE and worked there until now. He worked as a research fellow or visiting scholar in Hanyang University, S. Korea (2012–2013), Nanyang Technological University, Singapore (2013–2014) and University of Maryland, College Park, USA, (2018–2019). So far, he has coauthored over 190 peer-reviewed journal papers and applied more than 80 Chinese patents. His major interests include all-solid-state lithium/sodium batteries.

by a disproportionation reaction that generates O₂ and traps these molecules inside the Li₂O₂ particles, leading to particle inflation and the creation of a hollow structure.^[6] Interestingly, Luo et al. observed the unique discharge product Li₂O on the outer surface of the hollow particles, where excess O₂ came into direct contact with the discharge product.^[7] To gain insights into the battery system, the *in situ* differential electrochemical mass spectrometer (DEMS) instrument can be employed to measure the consumption and generation of various gases during battery operation. By comparing these measurements with the transferred charge, it becomes possible to determine the dominant electrochemical reaction equations in the battery system.

Despite the successful completion of the first all-solid-state Li-air battery by Kumar et al. in 2010,^[8] which consisted of a polymer/ceramic hybrid electrolyte, a carbon-based composite air cathode, and a lithium metal anode, there is still significant room for improvement in terms of ionic conductivity of the electrolyte, energy efficiency, cycle life, and interface stability. The technical challenges were also compounded by the unclear bulk ionic transport and transition mechanisms of inorganic solid electrolytes, the slow cathode reaction kinetics, the solid contact between the electrode and the electrolyte, as well as the active material and the cathode, the dendrite formation, and the instability of air when utilizing lithium metal anodes.^[9] The literatures on Li-air batteries have focused predominantly on the liquid Li-air battery system, with a particular emphasis on the liquid electrolyte, cathode material, and redox mediator employed in the liquid battery.^[3c,10] However, the area of the solid-state Li-air batteries (SSLABs) system is lack of systematically summarizing due to it's a relatively nascent field. As a result, the objective of this review is to bridge this gap in the literature, with a focus on the solid-state electrolyte, air cathode,

and interface issues. The reports include comprehensive assessment of the present state of solid-state Li-air batteries, comparison of existing systems, and evaluation of various battery modification strategies.

2. Solid Electrolytes for Lithium-Air Batteries

As a critical component in solid-state Li-air batteries, the performance of the solid electrolyte directly affects the performance of the battery. For the determination of the performance of solid electrolytes, the following criteria are generally examined: 1) high Li⁺ ionic conductivity and low electronic conductivity; 2) wide electrochemical window; and 3) good thermal and chemical stability. Currently, some solid polymer electrolytes and inorganic ceramic electrolytes have been used to fabricate solid-state Li-air batteries.^[11] A summary of recent research on Li-air or Li–O₂ batteries employing solid electrolytes can be found in Table 1, which presents information on the type of electrolyte used in the battery, ionic conductivity, operating environment, and battery electrochemical performance. These studies will be discussed in detail in subsequent sections. Currently, it appears that oxide electrolytes or oxide-polymer composite electrolytes are favored for solid-state lithium-air battery systems. This preference arises from their excellent stability to air, relatively high ionic conductivity, and the ability to adjust interfacial contacts.

2.1. Polymer solid electrolytes

In 1973, Fenton et al. firstly reported the ionic conductivity of poly(ethylene oxide) (PEO) with alkali metals.^[26] Since then, solid

Table 1. Summary of recent report on solid-state Li-air (O₂) batteries with different electrolytes,

Solid electrolytes	Operating environment	Is all-solid-state?	Ionic conductivity [$\times 10^{-4}$ S cm ⁻¹]	Initial discharge capacity [mA h g ⁻¹]/current density [mA g ⁻¹]	Cyclic performance/current density [mA g ⁻¹]/cycle capacity [mA h g ⁻¹]	Ref.
LAGP	Ambient air, RT	Yes	2	7850/10	2/200/1000	[12]
LAGP	Ambient air, RT	Yes	2	2800/200	10/400/1000	[13]
PEO-based SPE	Ambient air, 80 °C	No	–	–	40/–/220	[14]
LAGP	Ambient air, RT	Yes	2.1	4587/200	10/400/1000	[15]
Germanium film coated LAGP	Ambient air, RT	No	2.1	–	30/200/1000	[16]
Ultra fine LAGP	Ambient air, RT	Yes	3.9	–	27/400/1000	[17]
LATP	Ambient air, RT	Yes	0.71	–	50/–/5000	[18]
LLZTO/GPE	Oxygen, RT	No	10.6	7540/312.5	194/312.5/1250	[19]
Ultra-dry PVDF-HFP	Oxygen, RT	No	0.79	2800/400	60/400/1000	[20]
Adjustable-porosity plastic crystal electrolyte	Oxygen, RT	Yes	3.87	5963/200	130/200/500	[21]
Zeolite-based thin membrane	Ambient air, RT	Yes	2.67	12020/500	149/500/1000	[22]
LiIL-MOF	Oxygen, 60 °C	No	6.74 (30 °C)	3150/100	110/100/500	[23]
PEGMEM@LLZTO	Oxygen, RT	Yes	3.16	21733/167	68/167/833	[24]
LGPS/PEO	Ambient air, RT	–	5.2	–	1000/1000/1000	[25]

state polymer electrolytes (SPEs) have attracted special attentions. The greatest advantage of solid polymer electrolytes over inorganic ceramic electrolytes is their good flexibility, which allows them to be used in flexible wearable devices. Peng et al.^[27] and Zhang et al.^[28] reported the development of cable-like all-solid-state Li-air batteries using polymer electrolytes, as shown in Figure 1.

Migration of solvated Li^+ occurs due to the movement of molecular chains in the polymer. The migration capacity depends on the amount of freely movable Li^+ and the Li^+ mobility.^[29] The migration ability of Li^+ in polymers is much less than in organic electrolytes and needs to be improved by modification. Common modification methods include adding inorganic fillers and increasing the working temperature. Among them, the addition of inorganic fillers including inert fillers and active fillers with higher ionic conductivity, is a general practice. Currently, the main polymer electrolytes used in solid-state Li-air batteries are PEO, polyacrylonitrile (PAN), polyethylene glycol dimethyl ether (PEG-DME), polyvinylidene fluoride hexafluoropropylene (PVDF-HFP), and poly(methyl methacrylate) doped with polyphenylethylene (P(MMA-St)).^[2,30]

PEO-based polymer electrolytes were the first solid polymer electrolytes studied and consist of PEO compounded with the lithium salt LiX , denoted by PEO-LiX , where X denotes the anion in the lithium salt. PEO-LiX polymers are semi-crystalline and therefore have a low ionic conductivity of less than $10^{-6} \text{ S cm}^{-1}$ at room temperature.^[31] However, an increase of the temper-

ature to $80\text{--}90^\circ\text{C}$ turns the polymer into a viscous liquid, and its ionic conductivity suddenly increases to 1 mS cm^{-1} . In polymers, anions tend to have a higher mobility than Li^+ , which leads to a decrease in the Li^+ transference number. The introduction of lithium salts containing large organic anions, such as lithium bis(trifluoromethanesulfonyl)imide (LiTFSI) can alleviate this situation while acting as a plasticizer to further improve the ionic conductivity and flexibility of the polymer.^[32]

To improve the performances of PEO-LiX solid polymer electrolytes, a lot of research has been conducted. Tsuchida et al.^[33] obtained a polymer with intramolecular hydrogen bonds by mixing PEO with PMMA (Poly(methacrylic acid)). The ionic conductivity of LiClO_4 as a lithium salt can reach $1.3 \times 10^{-5} \text{ S cm}^{-1}$ at 60°C . A common modification method is by addition of inorganic ceramic powders,^[34] including insulating SiO_2 , Al_2O_3 , TiO_2 , and solid electrolyte powders such as garnet and NASICON-type ceramics with Li^+ conductivity.^[35] In 2011, Hassoun et al.^[36] prepared composite electrolyte membranes by adding ZrO_2 powder to $\text{PEO}_{20}\text{-LiCF}_3\text{SO}_3$ electrolyte. The electrolyte membranes achieved lithium ionic conductivity of 10^{-4} to $10^{-5} \text{ S cm}^{-1}$ at room temperature and were successfully used to assemble solid-state Li-air batteries. Compared with liquid organic electrolytes, PEO electrolytes have better stability against nucleophilic attack of Li_2O_2 , O_2^- , etc., and are therefore used to study the electrochemical processes in the cathode of solid-state Li-air batteries.^[36]

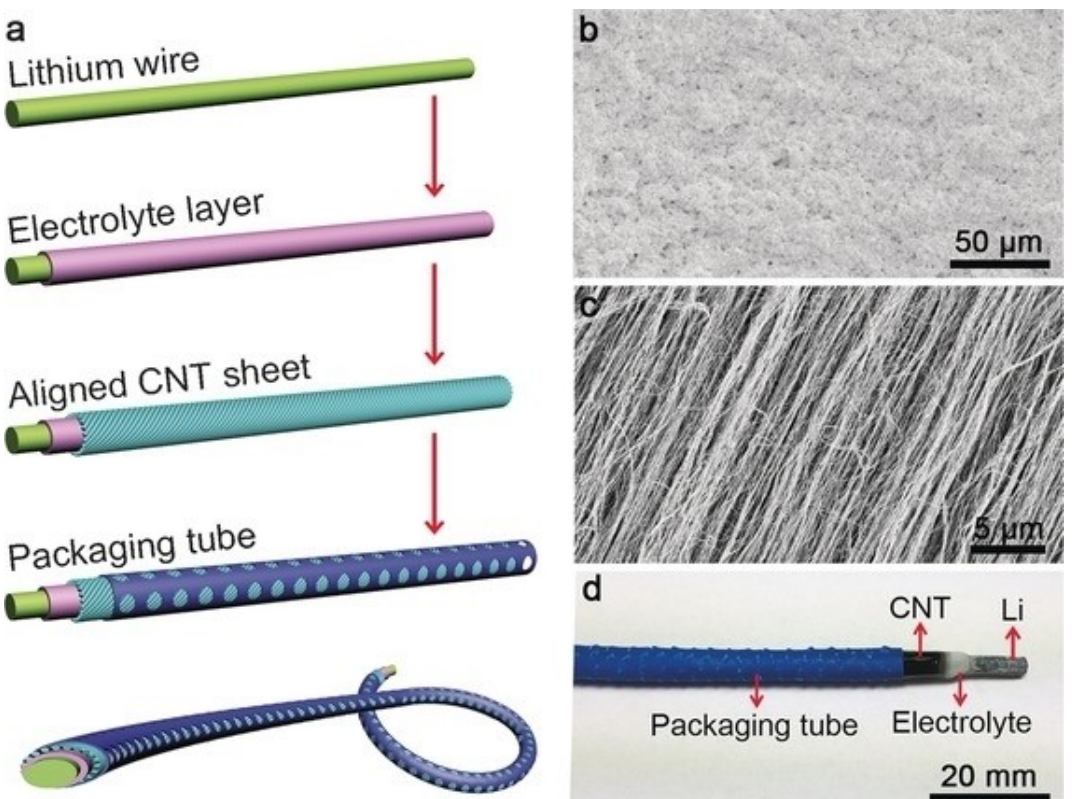


Figure 1. Schematic illustration of the fabrication and structure characterization of the fiber-shaped Li-air battery. a) A typical fabrication. b) SEM image of gel electrolyte coated on the Li wire. c) SEM image of aligned CNT sheet wrapped as the outer layer. d) Photograph of a fiber-shaped Li-air battery. Reproduced with permission from Ref. [27]. Copyright (2016) Wiley-VCH.

2.2. Oxide solid electrolytes

Oxide solid electrolytes usually derived from precursor powder by primary calcination of raw materials following by high temperature sintering to obtain a stiff and brittle electrolyte. Due to its intrinsic stability with exposure to the air, the steps of material preparation, battery manufacturing, and encapsulation could be significantly simplified, thus improving entire battery safety appreciably.^[37] In addition, the high thermal stability of these electrolytes allows the battery to maintain safe operation and performance stability over a range of temperatures, reducing the need for accessory modules such as thermal management and power electronics in the battery module, thereby significantly reducing the weight, cost, and complexity of the battery pack. The crystal configuration of oxide solid electrolytes consists of a primary and a secondary atomic structure.^[38] The primary atomic structure consists of a three-dimensional (3D) network of oxidized polyhedra. The secondary atomic structure is located within the pores of the 3D network and consists of a permeable grid of occupied/unoccupied sites. To move from one site to another, the cation needs to leap over the “bottleneck” of the oxidation polyhedra with an activation energy varying from 0.2 to 0.5 eV. Three of the most common oxide solid electrolytes are briefly described below, including perovskite, NASICON-type, and garnet-type electrolytes, respectively.

The general chemical formula of a perovskite solid electrolyte is ABO_3 ($\text{A}=\text{Ca}, \text{Sr}, \text{La}; \text{B}=\text{Al}, \text{Ti}$, etc.), which belongs to the cubic unit cell and the $\text{Pm}/\text{3 m}$ space group. A-type atoms are generally at the apex angle of the cubic unit cell, B-type atoms are in the center, and the remaining oxygen atoms are in the face-centered position. In this way, the type A atoms are at the 12-coordination center, and the type B atoms are at the 6-coordination center. Lithium-ions are introduced by heterovalent doping. The introduction of lithium-ions not only increases the lithium content of the compound, but also increases the vacancy concentration. Such doping leads to the ordering of lithium-ions and increased vacancies at c -axis, which greatly increases the lithium ionic conductivity in this direction. At room temperature, lithium-ions can jump through the octahedral bottleneck formed by oxygen atoms in the AB plane and transiting through adjacent vacancies. The octahedral bottleneck can be widened by using large-diameter rare earth elements and alkaline earth elements, thereby further improving lithium ionic conductivity. At present, among the discovered perovskite solid electrolytes, the highest ionic conductivity belongs to $\text{Li}_{0.34}\text{La}_{0.56}\text{TiO}_3$, whose ionic conductivity is about 10^{-3} Scm^{-1} with overall ionic conductivity of $7 \times 10^{-5} \text{ Scm}^{-1}$.^[39] The most significant problem with perovskite solid electrolytes is that tetravalent titanium reacts with lithium resulting in reduction. In addition, the long-term storage stability of perovskite solid electrolytes also needs to be improved. Zhao et al.^[40] reported a novel Li-rich anti-perovskite with a general formula of Li_3OX ($\text{X}=\text{Cl}, \text{Br}$). In this structure, lithium-ions occupy the top corner of the octahedron and connect with the oxygen ions (B-site) at the center of the octahedron, while the halogen element (A-site) is in the center of the dodecahedron.

The benefits of anti-perovskite solid electrolytes are lithium-rich elements and light weight. More noticeably, the ionic conductivity of Li_3OCl and $\text{Li}_3\text{OCl}_{0.5}\text{Br}_{0.5}$ at room temperature are as high as $0.85 \times 10^{-3} \text{ Scm}^{-1}$ and $1.94 \times 10^{-3} \text{ Scm}^{-1}$, respectively. Further research found that Li_2OHX with an inverse perovskite structure can also be used as a solid electrolyte, and it is also stable with lithium metal. Substituting fluoride anions for hydroxide ions results in compounds with the chemical formula $\text{Li}_2(\text{OH})_{0.9}\text{F}_{0.1}\text{Cl}$. The electrochemical window of this solid electrolyte is as high as 9 V. However, according to density functional theory (DFT) calculations, the Li_3OX tends to decompose, this encompasses the efforts of investigating in the stability of anti-perovskite solid electrolytes and the improvement of ionic conductivity.

NASICON-type solid electrolyte was first proposed in 1976 by Goodenough and Hong et al.^[41] It is based on $\text{NaZr}_2(\text{PO}_4)_3$ solid solution with partial replacement of P^{5+} by Si^{4+} to form a 3D sodium fast ionic conductor with the general formula $\text{Na}_{1+x}\text{Zr}_2\text{Si}_x\text{P}_{3-x}\text{O}_{12}$ ($0 \leq x \leq 3$), where $\text{Na}_3\text{Zr}_2\text{Si}_2\text{PO}_{12}$ exhibits a high ionic conductivity of $6.7 \times 10^{-4} \text{ Scm}^{-1}$ at room temperature and 0.2 Scm^{-1} at 300°C when $x=2$.^[41,42] The NASICON solid electrolyte has a covalent skeleton structure consisting of interconnected polyhedra, where the ZrO_6 octahedra and PO_4/SiO_4 tetrahedra are connected at common vertices to form a 3D skeleton. Na^+ ions and vacancies are located at the skeleton gap sites and conduct along the 3D channels formed by these gaps. As shown in Figure 2, NASICON electrolytes exist in both hexagonal phase (space group R-3c) and monoclinic phase (space group C2/c) structures.^[43] It is commonly believed that $\text{Na}_{1+x}\text{Zr}_2\text{Si}_x\text{P}_{3-x}\text{O}_{12}$ exhibits a monoclinic phase when $1.8 \leq x \leq 2.2$, and the remaining components exhibit a hexagonal phase structure.^[42,44] Also, the change in temperature causes a transition in the phase structure, and when the temperature is heated to 150 – 180°C , the monoclinic phase transforms into the hexagonal phase.^[45]

Na^+ in $\text{Na}_3\text{Zr}_2\text{Si}_2\text{PO}_{12}$ can be replaced by Li^+ ions to obtain NASICON type lithium-ion solid electrolyte. However, since the Li^+ radius (0.68 \AA) is smaller than that of Na^+ radius (0.97 \AA), the direct introduction of Li^+ into the high coordination position of Na^+ will easily lead to the collapse of the framework structure, which is not conducive to Li transport. Therefore, the ionic conductivity of $\text{Li}_3\text{Zr}_2\text{Si}_2\text{PO}_{12}$ obtained directly by solid-phase ion exchange using high-temperature molten salt is three orders of magnitude lower than that of $\text{Na}_3\text{Zr}_2\text{Si}_2\text{PO}_{12}$. In this case, suitable ions can be used to replace the skeletal ions to construct a proper Li coordination environment and stabilize the framework structure of the precursor to improve the ionic conductivity. In 1989, Aono et al.^[46] prepared a NASICON-type lithium-ion solid electrolyte $\text{Li}_{1.3}\text{Al}_{0.3}\text{Ti}_{1.7}(\text{PO}_4)_3$ (also known as LATP) with a high ionic conductivity of $7 \times 10^{-4} \text{ Scm}^{-1}$ at room temperature and 0.09 Scm^{-1} at 300°C by replacing Zr^{4+} with Ti^{4+} and doping it with an appropriate amount of Al^{3+} . Subsequently in 1992, Aono et al.^[47] used Ge^{4+} instead of Zr^{4+} , also doped with an appropriate amount of Al^{3+} , to obtain a NASICON-type lithium-ion solid electrolyte $\text{Li}_{1.5}\text{Al}_{0.5}\text{Ge}_{1.5}(\text{PO}_4)_3$ (also known as LAGP) with a room temperature ionic conductivity of $2.4 \times 10^{-4} \text{ Scm}^{-1}$. NASICON-type lithium-ion solid

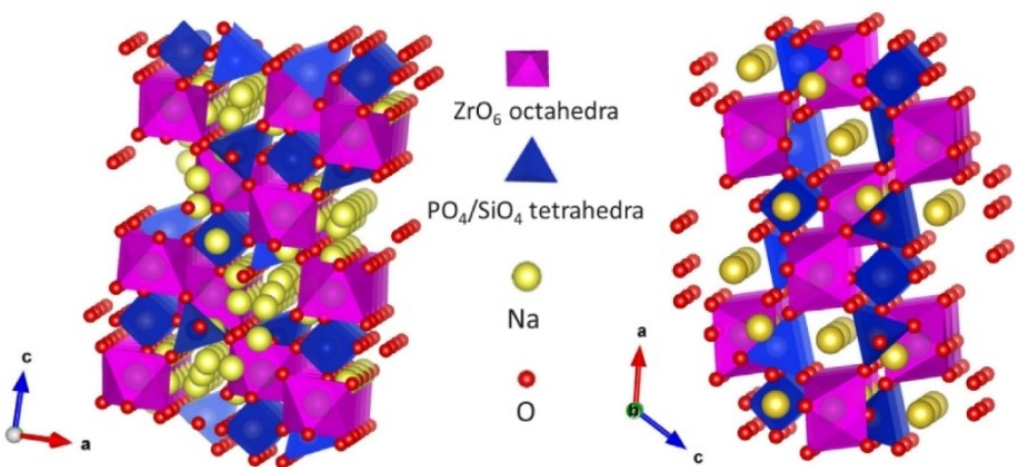


Figure 2. Crystal structure of NASICON-type electrolyte. Reproduced with permission from Ref. [43]. Copyright (2018) Elsevier.

electrolytes therefore include two main types, LATP and LAGP. However, the tendency for Ti^{4+} and Ge^{4+} to be reduced at low potentials has led to NASICON-type lithium-ion solid electrolytes being unstable to lithium metal, thus limits the application of these electrolytes. It has been reported that the use of solid electrolytes containing tetravalent germanium (Ge) is more stable, but there are still reports that tetravalent Ge will also react with lithium and be reduced to elemental and bivalent Ge.

Since Thangadurai et al.^[48] firstly reported the garnet-type solid electrolyte $Li_5La_3M_2O_{12}$ ($M=Ta, Nb$), it has received much attentions due to its chemical stability for lithium metal electrode and its wide electrochemical window. In 2007, Murugan et al.^[49] replaced M with Zr and increased the Li concentration to achieve a garnet-type electrolyte $Li_7La_3Zr_2O_{12}$ (also known as LLZO) with a higher ionic conductivity of $3 \times 10^{-4} \text{ Scm}^{-1}$ at room temperature. As shown in Figure 3, LLZO

electrolytes can be divided into two structures, i.e., the tetragonal phase (space group $I4_1/acd$) and the cubic phase (space group $Ia-3d$). Lithium exists in three different sites in the tetrahedral phase, with $Li1$ occupying position $8a$ in the tetrahedral gap, $Li2$ occupying position $16f$ in the ortho-octahedral gap and $Li3$ occupying position $32g$ in the partial-octahedral gap, showing an ordered distribution of lithium-ions.^[50] In contrast, there are two different sites for lithium in the cubic phase, with $Li1$ occupying the $24d$ position in the tetrahedral gap and $Li2$ occupying the $96h$ position in the eccentric octahedral gap, where the lithium-ions show a disordered distribution, making ion migration easier and thus exhibiting higher ionic conductivity.^[51] Stabilization of the cubic phase at room temperature is therefore the key to the synthesis of LLZO-based electrolytes with high ionic conductivity. It is worth noting that garnet-type electrolytes tend to react with CO_2 and H_2O in the air and a layer of Li_2CO_3 impurities is generated on the surface, leading to a decrease in their affinity for the electrode.^[52] Sun et al.^[53] constructed all-solid-state Li-air batteries based on LLZTO ceramic solid electrolyte and carbon-based composite solid-air cathode, and the evolution of Li-air battery performances and products were investigated.

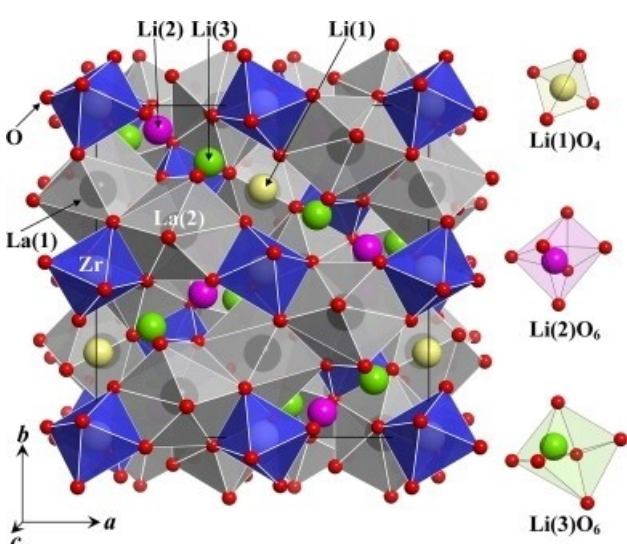


Figure 3. Crystallite structure of tetragonal LLZO. Reproduced with permission from Ref. [50]. Copyright (2009) Elsevier.

2.3. Sulfide solid electrolytes

Sulfide solid electrolytes are derived from oxide solid electrolytes by replacing the oxygen ions in the oxide with sulfur ions of larger ionic radius, which can form a wider ion conducting pathway. In addition, the strong polarization of sulfur ions and their weaker binding ability to lithium-ions gives lithium-ions a higher mobility, so sulfide solid electrolytes tend to exhibit higher ionic conductivity compared to oxide solid electrolytes.^[54] Meanwhile, sulfide solid electrolytes have better mechanical ductility than oxide electrolytes and dense interfaces can be easily achieved by cold pressing.^[55] Sulfide solid electrolytes can be mainly classified into two types, binary sulfide and ternary sulfide according to the type of synthetic

raw materials.^[56] Binary sulfides are mainly synthesized from M_2S ($M=Li, Na$) and P_2S_5 as raw materials, while ternary sulfides are mainly synthesized from M_2S ($M=Li, Na$), P_2S_5 and MS_2 ($M=Si, Ge, Sn$) or MX ($M=Li, Na; X=Cl, Br, I$). Since sulfide electrolytes tend to contain P–S bonds with weak bonding energy, the vast majority of sulfide solid electrolytes exhibit poor air stability and react with H_2O in the gas to form H_2S gas.^[57] The sulfide raw materials used are also less stable to humid air, so the sulfide solid electrolytes are generally synthesized and stored under inert atmosphere. Nowadays, in order to improve the air stability of sulfide solid electrolytes, P is partially or even completely replaced by other elements, and the air stability of the obtained electrolytes is greatly enhanced, such as $Li_{3.06}P_{0.98}Zn_{0.02}S_{3.98}O_{0.02}$, Na_3SbS_4 .^[58]

In 2011, Kanno et al.^[59] synthesized the ternary sulfide solid electrolyte $Li_{10}GeP_2S_{12}$ using Li_2S , GeS_2 , and P_2S_5 under argon atmosphere, and its crystal structure is shown in Figure 4. The $(Ge_{0.5}P_{0.5})S_4/PS_4$ tetrahedra, LiS_4 tetrahedra and LiS_6 octahedra form a 3D skeleton structure. The LiS_4 tetrahedra at positions 16 h and 8f are co-linked along the c-axis to form a one-dimensional zigzag lithium-ion conduction path. Due to the isotropic transport of lithium-ions, the $Li_{10}GeP_2S_{12}$ solid electrolyte demonstrates an ultra-high room temperature ionic conductivity of 12 mScm^{-1} . It is the first time when the ionic conductivity of a solid electrolyte surpasses that of a conventional liquid electrolyte, and it is indeed a milestone for the solid electrolyte. However, the introduction of Ge^{4+} led to the lack of stability of $Li_{10}GeP_2S_{12}$ to lithium metal anodes. And the first $Li_{10}GeP_2S_{12}$ -based battery assembled by Kanno et al. also used indium metal anodes with higher potentials, thus

improving the interfacial stability of $Li_{10}GeP_2S_{12}/Li$ is the key to realize $Li_{10}GeP_2S_{12}$ -based solid-state batteries.

Although sulfides have very high ionic conductivity and good interfacial physical contact, their chemical instability in presence of air limits their application in solid-state Li-air batteries. If the sulfide electrolyte could withstand the instability to water in the air and instability to lithium metal, the potential application in Li-air batteries would be greatly improved. While pure sulfide electrolytes are still flawed, composite solid-state electrolytes containing sulfide can enable high performance Li-air batteries at room temperature. Kondori et al. reported a Li-air battery using a ceramic-poly(ethylene oxide)-based composite solid-state electrolyte, which was found to perform a four-electron redox reaction through the formation and decomposition of Li_2O (Figure 5).^[25] The composite electrolyte embedded with $Li_{10}GeP_2S_{12}$ nanoparticles showed a high ionic conductivity ($5.2 \times 10^{-4}\text{ Scm}^{-1}$). The authors used this solid electrolyte and catalyst Mo_3P to achieve a four-electron reaction with 1000 reversible cycles at room temperature under the limited capacity of 1000 mAh g^{-1} . The formation of LiO_2 and Li_2O_2 was observed during the first 15 min, after which Li_2O became the main discharge product. During this process, Li_2O_2 is isolated below Li_2O in the absence of O_2 and comes into direct contact with the most favorable cathode for electron transfer, which allows Li_2O_2 to undergo a two-electron reduction to Li_2O . Thus, combining two two-electron reactions (O_2/Li_2O_2 and Li_2O_2/Li_2O) yields a highly desirable four-electron Li-air chemistry. Moreover, the results of this study also demonstrate that a Li-air battery system based on this electrolyte and a four-electron reaction can realize an expected specific energy of greater than 1000 Wh kg^{-1} (bulk energy density of 1000 Wh L^{-1}), which

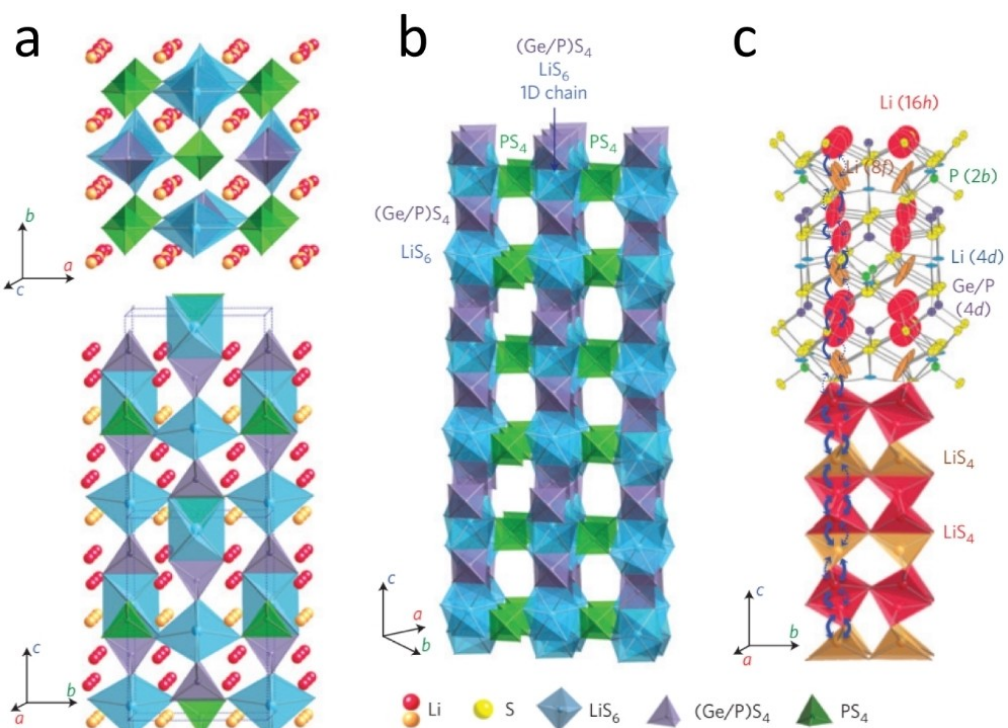


Figure 4. Crystal structure of $Li_{10}GeP_2S_{12}$. Reproduced with permission from Ref. [59]. Copyright (2011) Springer Nature.

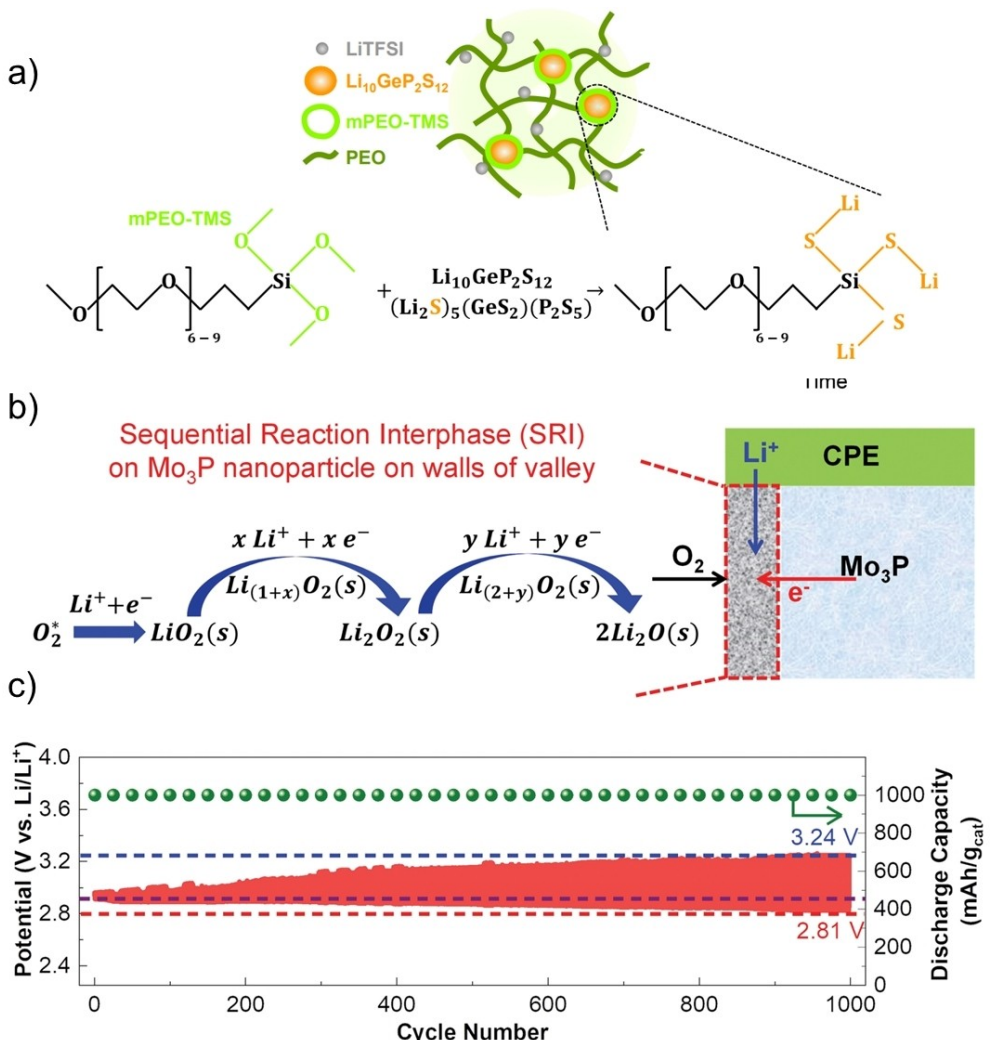


Figure 5. a) Schematic illustration of CPE configuration. Bond formation between S atoms in the LGPS and the Si atoms in the mPEO-TMS and their configuration in the PEO-LiTFSI matrix. b) Detailed reaction mechanism for an SRI on a Mo_3P nanoparticle surface. c) Galvanostatic cyclic performance over 1000 cycles at a constant current density of 1 A g^{-1} and a limited capacity of 1 Ah g^{-1} . Reproduced with permission from Ref. [25]. Copyright (2023) The American Association for the Advancement of Science.

would provide a much higher battery energy density than current lithium-ion technology.

2.4. Others

In addition to the widely studied solid electrolytes previously mentioned, novel metal-organic framework (MOF) materials as well as 3D covalent organic framework (COF) materials have also been shown to be used to prepare high-performance solid-state Li-air batteries. Wang et al. prepared MOF materials with excellent electron and ionic conductivity tunability, which were used as both solid-state electrolyte and solid-air cathode for Li-air batteries, and constructed a high-safety and long-life light-assisted solid-state Li-air battery (Figure 6a).^[60] MOF materials are also known as coordination polymers or porous coordination polymers. They are formed by the coordination bonds between metal ions or clusters and organic ligands, resulting in

highly ordered crystalline structures. MOF materials exhibit porosity in their structure and often display highly ordered pores and surface areas, which gives them significant potential for diverse applications. In contrast to conventional solid-state electrolyte materials, MOF solid electrolytes exhibit high ionic conductivity, high electrochemical stability, and high environmental adaptability. Compared with the complex structure and composition of conventional solid-state air cathode (containing electron conductor skeleton, ion conductor layer, gas diffusion layer, etc.), this work realizes a solid-state air cathode with good electron, ion and gas transport at the same time using a single MOF material. The solid-state Li-air battery based on this design exhibits a high energy efficiency of 94.2% and a long cycle life of 320 cycles. Furthermore, Wang et al. synthesized 3D COF-based solid electrolyte materials using microwave-assisted method and revealed the transport mechanism of lithium ions in the material skeleton (Figure 6b).^[61] The conduction mechanism of lithium ions within its pore channels was probed using

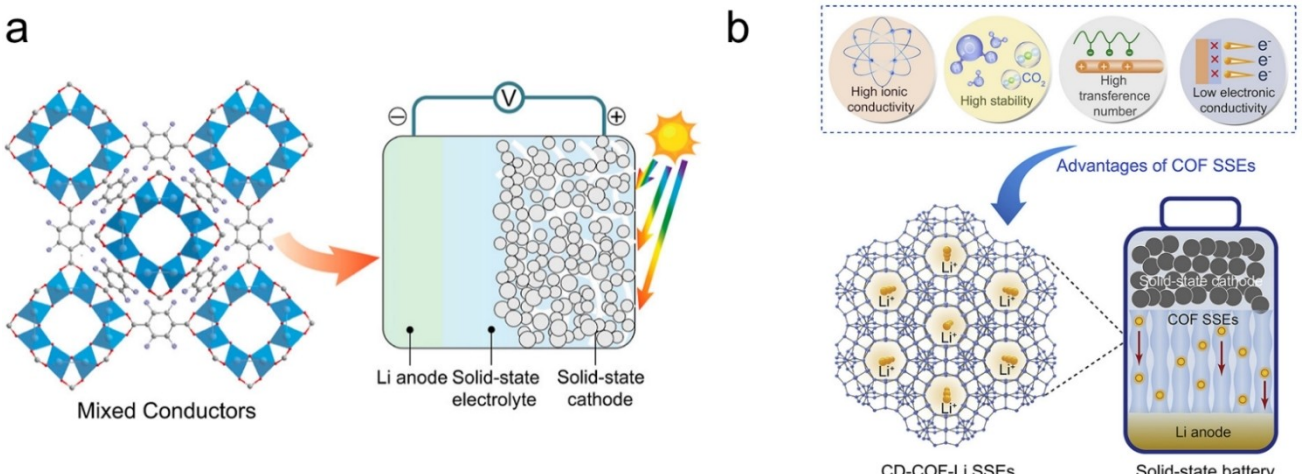


Figure 6. a) Schematic of MOF-based mixed conductors and a photo-assisted solid-state Li–O₂ battery. Reproduced with permission from Ref. [60]. Copyright (2023) American Chemical Society. b) Schematic and features of the COF solid electrolyte in the solid-state battery. Reproduced with permission from Ref. [61]. Copyright (2023) Elsevier.

solid-state nuclear magnetic resonance (NMR) technique. This COF solid-state electrolyte exhibited ionic conductivity up to $2.7 \times 10^{-3} \text{ Scm}^{-1}$ and excellent electrochemical stability due to the abundant ion transport channels, unique skeleton flexibility and short interfacial transport impedance. As a result, both solid-state Li–O₂ and solid-state Li-metal batteries employing COF solid electrolytes exhibit superior discharge capacity, rate performance, and cycle life, providing new ideas for the diversified design of lithium-ion conductors for solid-state Li-air batteries.

3. Interfacial Challenges in Solid-State Li-Air Batteries

In contrast to batteries using conventional liquid electrolytes, the contact between the components inside solid-state Li-air batteries is a solid-solid contact. This includes the active material/cathode material interface, the anode/electrolyte interface and the cathode/electrolyte interface. The active material/cathode material interface is the oxygen/electron conductor/ion conductor “triple-phase” interface in solid-state Li-air batteries, which has an important influence on the formation and decomposition of discharge products. The cathode/electrolyte and anode/electrolyte interface resistance is an important component of the internal resistance of the battery, which affects the transport of lithium-ions inside the battery.

3.1. Interfacial issues between lithium anode and solid electrolyte

The anode of SSLAB is a critical component to achieve superior battery performance, which directly affects the energy density, cycle life and safety of the battery. Unlike conventional liquid

lithium-ion batteries, SSLABs show great potential to use lithium metal as the anode rather than graphite or silicon-carbon materials. Lithium metal is a lightweight, high-energy-density material that can store more energy and has a higher energy density compared to traditional lithium-ion batteries. Additionally, the lithium metal electrode can improve electrical conductivity, reduce the drift and polarization of lithium ions as well as diminish the overall internal resistance of the battery.

However, there are still many issues with the lithium anode in SSLAB. For example, lithium metal is prone to dendrite growth and lithium metal deposition during charging and discharging, which may cause safety problems such as short circuit, overheating and fire of the battery. Lithium dendrites can form where the lithium anode is in contact with the solid electrolyte and grow along the grain boundaries and interconnected micropores in the solid electrolyte, eventually leading to short-circuit failure of the battery.^[62] Besides, some solid electrolytes can have redox reactions with lithium metal, leading to degradation of electrolytes and battery failure. In addition, the interface contact between the lithium metal and the solid electrolyte is a point-to-point solid-solid contact, which increases the internal resistance of the battery compared to the liquid battery. The volume expansion of the lithium metal during the stripping/plating process further affects the contact between the electrodes and the electrolyte, causing a decrease in cell efficiency and cycle life. More research is needed on the dendritic and interfacial issues associated with the use of lithium metal anode. For the above-mentioned problems regarding the lithium anode, several solutions are recommended as follow.

First, increasing the relative density of the solid electrolyte and reducing the internal porosity can inhibit the growth of lithium dendrites. Second, heat treatment of the anode, such as *in situ* melting of lithium on the surface of the solid electrolyte LAGP, has been shown to reduce interfacial impedance and enhance interfacial stability.^[63] This is due to the fact that

molten liquid lithium can make further contact with the rough electrolyte surface. Moreover, the use of alloy anodes can also reduce the interfacial impedance and inhibit the growth of lithium dendrites to some extent. However, the effect varies depending on different electrolytes and different alloy anodes employed. Last, introducing a lithiophilic thin-film intermediate layer between the anode and the electrolyte is also an effective way to reduce lithium dendrites and lower the interfacial impedance. Thin films can generally be introduced by magnetron sputtering, evaporative bonding films, atomic layer deposition, and chemical vapor deposition. Currently, a series of thin film layers have been introduced between the solid electrolyte and the lithium anode, including Si, Al, Al_2O_3 , Ge, Au, ZnO, or polymers such as PEO and PVDF-HFP.^[16,64] Garnet-type solid-state electrolytes are known for their high lithium ionic conductivity and good stability to lithium, but the contact impedance between these electrolytes and lithium is very high. Recently, it has been reported that the introduction of transition layers that can form an alloy with Li can improve the interfacial contact between the garnet electrolyte and metallic Li and reduce the Li/electrolyte interface resistance. These alloyed anodes include Li–Si,^[64a] Li–Ge,^[64b] Li–Al,^[64d] Li–Zn,^[64c] and Li–Au.^[65] For example, as shown in Figure 7, Luo et al. grew a Si film on the surface of LLZ material by plasma-enhanced chemical vapor deposition (PECVD).^[64a] The LLZ surface with good wettability to metallic Li was obtained by the reaction between Si and metallic Li and the Li/LLZ interface resistance was reduced from $925 \Omega \text{cm}^2$ to $127 \Omega \text{cm}^2$. The thin film buffer layer also improves the chemical stability between the lithium metal and the electrolyte.

Liu et al.^[16] used ion beam sputtering to deposit amorphous germanium nanofilms on the side of the NASICON-type electro-

lyte LAGP after surface treatment and assembled solid-state Li-air cells for electrochemical performance testing. As shown in Figure 8, the use of such germanium nanofilms not only effectively alleviated the problem of reduced tetravalent germanium in LAGP, but also promoted the electrolyte-electrode contact, reduced the interfacial impedance, and significantly improved the cell cycle life.

Besides, Gu et al.^[66] prepared a polymer electrolyte buffer layer on the oxide electrolyte surface using an *in situ* polymerization method and applied it to assemble solid-state Li–O₂ batteries. This design successfully improved the interfacial stability and interfacial wettability of the lithium metal and electrolyte, which significantly enhanced the cyclic performance as well as the actual specific capacity of the solid-state Li–O₂ battery. A noteworthy discovery was made by Shao et al.,^[67] who successfully enhanced the interfacial connection between garnet-type electrolyte and Li anode using a simple technique involving the use of a pencil to draw a graphite-based soft interface.

In general, solving the stability issues related to lithium metal has become the primary concern within lithium battery systems. The current understanding of the stability of lithium metal protected by solid electrolytes is still very limited. Reversible energy storage requires lithium to be reversibly dissolved (discharged) and deposited (charged) on the anode surface with a high Coulombic efficiency. It has been demonstrated that the chemical and morphological instability of lithium metal anode can be minimized by using solid electrolytes. Thus, anodes for solid-state Li-air batteries present multiple challenges that need to be addressed through research in material design and electrochemical interface optimization.

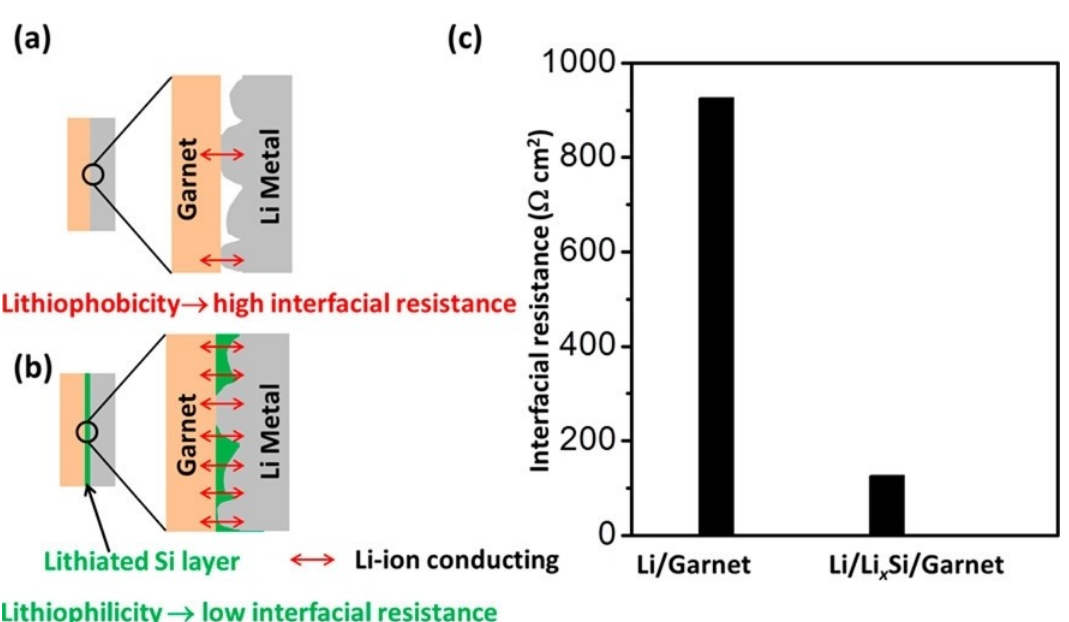


Figure 7. a) Lithiophobic garnet has poor contact with Li metal, which leads to a high interfacial resistance. b) The wettability of garnet is significantly improved due to the reaction between Li and Si and the *in-situ*-formed, lithiated Si can act as a Li-ion conducting layer. c) The wettability transition and the *in-situ*-formed, lithiated Si leads to the dramatic decrease of garnet/Li metal interfacial resistance from $925 \Omega \text{cm}^2$ (bare garnet) to $127 \Omega \text{cm}^2$ (Si-coated garnet). Reproduced with permission from Ref. [64a]. Copyright (2016) American Chemical Society.

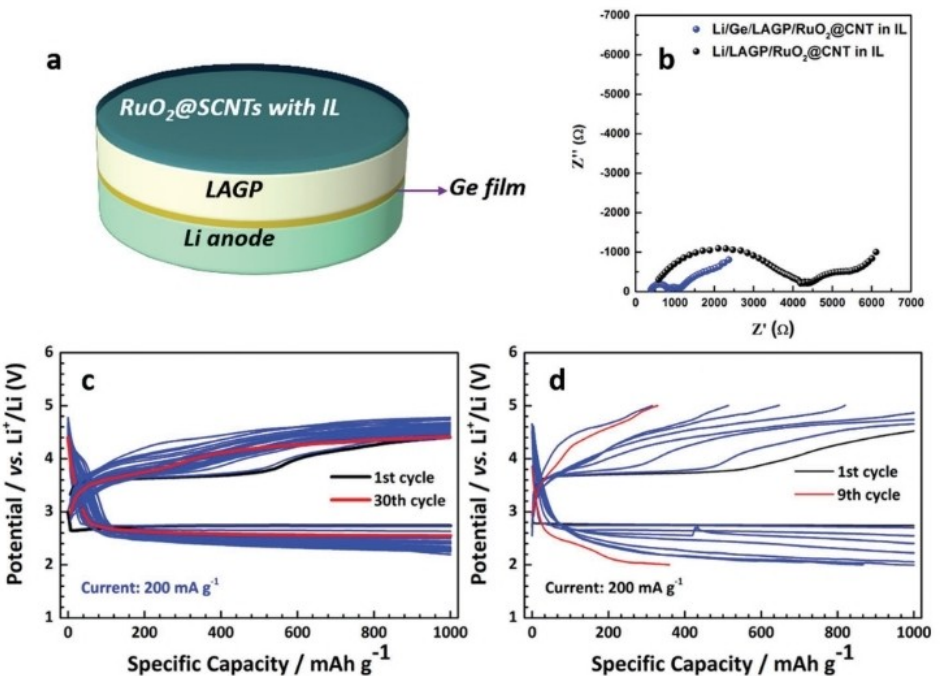


Figure 8. a) Schematic diagram of $\text{Li}/\text{Ge/LAGP/RuO}_2@\text{CNT}$ with ionic liquid battery. b) Nyquist plots of $\text{Li}/\text{LAGP/RuO}_2@\text{CNT}$ with IL and $\text{Li}/\text{Ge/LAGP/RuO}_2@\text{CNT}$ with IL. Cyclic performance of c) $\text{Li}/\text{Ge/LAGP/RuO}_2@\text{CNT}$ with IL battery and d) $\text{Li}/\text{LAGP/RuO}_2@\text{CNT}$ with IL battery. Reproduced with permission from Ref. [16]. Copyright (2018) Wiley-VCH.

3.2. Interfacial issues between air cathode and solid electrolyte

The location of the cathode reaction in solid-state Li-air batteries is at the active material/cathode material interface, and the construction of a “triple-phase” boundary with good electron, ion and gas transport properties is essential to promote the growth and decomposition of the product Li_2O_2 .

Zhong et al.^[68] investigated the decomposition process of the product Li_2O_2 in a solid-state $\text{Li}-\text{O}_2$ cell using in situ TEM technique, as shown in Figure 9. In the battery structure, MWCNT/ Li_2O_2 is the cathode, Si nanowires are the anode, and LiAlSiO_x coated on the Si surface is the solid electrolyte. After the battery starts charging, particle 1 near the solid electrolyte starts decomposing first, as shown in Figure 9(a, b). Particle 2 does not start decomposing at first until it starts to contact with

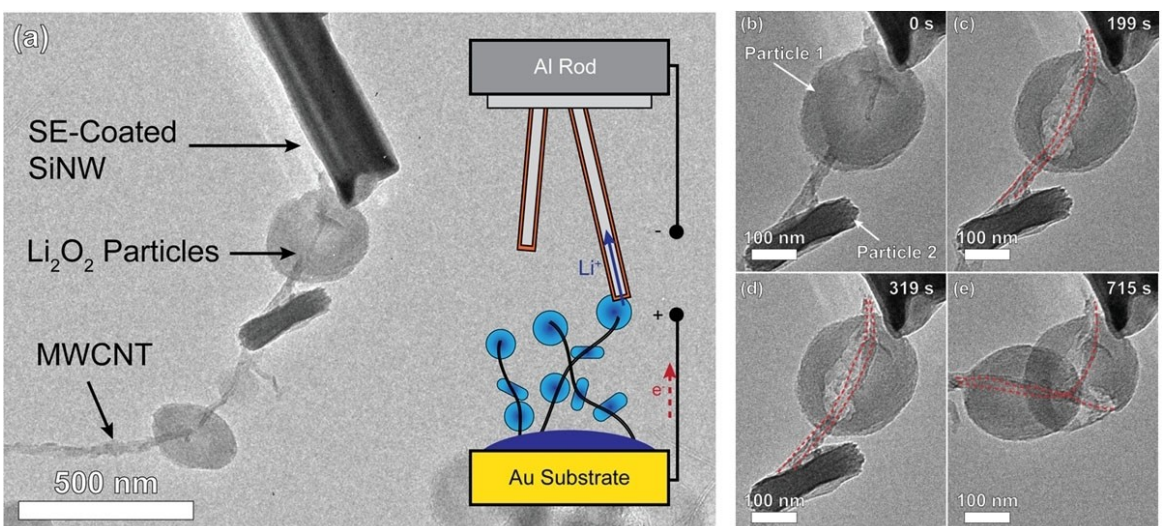


Figure 9. Oxidation of Li_2O_2 particles. a) Schematic illustration of the in situ TEM microbattery superimposed over a low-magnification TEM image of a SE-coated Si NW contacting a single Li_2O_2 particle. b) Higher-magnification TEM image of the particles in (a), showing a MWCNT bundle contacting two physically separated Li_2O_2 particles labeled as Particle 1 and Particle 2, respectively. c–e) Oxidation of Particles 1 and 2 during application of a 10 V potential to the MWCNT/ Li_2O_2 cathode against the Si NW anode. Reproduced with permission from Ref. [68]. Copyright (2013) American Chemical Society.

particle 1. This indicates that for the decomposition of Li_2O_2 , the reaction interface needs to be both electronically and ionically conductive, in which the solid air cathode needs to have a well-constructed "electron-ion-gas" interface.

For the cathode/electrolyte interface in solid-state Li-ion batteries, the high interfacial resistance is mainly caused by lattice mismatch, intermediate phase formation and space charge layer. The interface resistance can usually be reduced by interface design and the introduction of intermediate transition layers. In solid-state Li-air batteries, since the cathode component is mostly carbon material, the main influencing factors of the cathode/electrolyte interface resistance are lattice mismatch and intermediate phase formation, while the influence of the space charge layer is reduced. Currently, most solid-state Li-air batteries are designed with a separate cathode layer stacked with a separate solid electrolyte layer, and the separate cathode layer contains a large amount of electrolyte powder, which causes a large cathode/electrolyte interfacial resistance.^[69] By integrating the air cathode with the solid electrolyte layer to form a SSLAB with a composite structure, the interfacial resistance can be effectively reduced. Zhu et al.^[11b,18,70] constructed an integrated solid-state Li-air battery structure containing a dense LATP electrolyte layer and a porous LATP cathode layer. In a pure oxygen environment, this battery can be stably cycled for 100 and 20 cycles at a constant capacity of 1000 and 5000 mAh g^{-1} , respectively. However, due to the tetravalent titanium in the LATP solid-state electrolyte is easily reduced by lithium, an organic electrolyte is also added as a buffer layer between the electrolyte and the anode.

Li et al. introduced a solid electrolyte cathode assembly (SECA) composed of two distinct layers: a compact LAGP layer and a porous LAGP layer with a carbon coating.^[71] This SECA was efficiently manufactured through a simplified one-step sintering process. $\text{Li}-\text{O}_2$ batteries utilizing the SECA demonstrated a commendable discharge capacity of 0.48 mAh cm^{-2} when subjected to a current density of $5 \mu\text{A cm}^{-2}$. Another significant development was reported by Sun et al., who proposed a solid-state Li-air battery based on the garnet-type electrolyte LLZTO. In their study, they devised a composite

cathode comprising garnet powder, Li salt (LiTFSI), active carbon, and a polypropylene carbonate binder, aiming to minimize interfacial resistance. The battery exhibited an impressive discharge capacity of 20300 mAh g^{-1} carbon and underwent 50 cycles at a current density of $20 \mu\text{A cm}^{-2}$ and a temperature of 80°C , while maintaining a capacity of 1000 mAh g^{-1} (Figure 10).^[53] Chi et al. reported a solid-state Li-air battery using a lithium ion exchange molecular sieve membrane (LiXZM) as a solid-state electrolyte, in which the electrolyte is integrated with a lithium metal anode and a carbon nanotube cathode (Figure 11).^[22] The advantages of the molecular sieve include high chemical stability, which can inhibit the degradation of the solid-state electrolyte caused by lithium metal and air; excellent electrode-electrolyte interface, which can effectively reduce the interfacial contact impedance. Its unique *in situ* growth strategy overcomes the challenges of interfacial dendrite growth and poor stability.

Our group has also recently introduced an all-solid-state $\text{Li}-\text{O}_2$ battery based on a garnet electrolyte LLZTO (Figure 12).^[24] This work successfully prepared an integrated electrolyte-composite cathode structure by simple ball-mill mixing, *in situ* coating, and low-temperature sintering. The all-solid-state $\text{Li}-\text{O}_2$ battery assembled with this structure has a great initial discharge capacity ($13.04 \text{ mAh cm}^{-2}$) and an enhanced cycling stability. The results of battery testing, XPS analysis, DEMS analysis, and DFT calculations jointly indicate that an integrated structure is one of the best strategies to achieve a high-performance all-solid-state $\text{Li}-\text{O}_2$ battery. In the field of lithium batteries, DFT calculations play a crucial role in understanding the electronic structure, lithium-ion diffusion pathways, stability of intercalation compounds, interfaces, and redox reaction mechanisms in lithium batteries, thereby enhancing battery performance. It is a powerful tool, helping researchers to better understand battery materials and electrochemical processes, and guiding the design of more efficient, stable, and sustainable lithium-ion batteries. Particularly, in this case, DFT calculations were conducted to verify the beneficial impacts of the integrated cathode CNT@LLZTO on discharge/charge processes and to gain insights into the ORR/OER mechanisms during

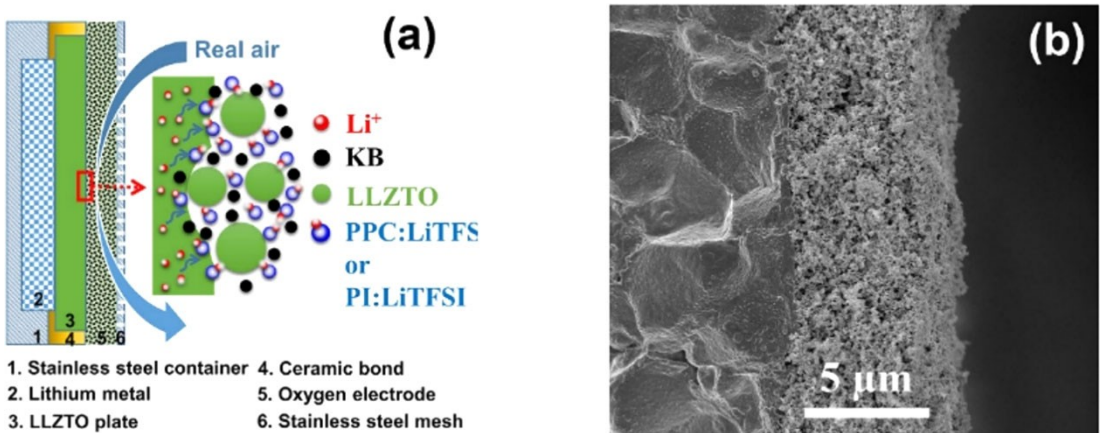


Figure 10. a) Schematic image of the composite solid state air cathode. b) Cross-section SEM image of a typical composite cathode/LLZTO interface. Reproduced with permission from Ref. [53]. Copyright (2017) Springer Nature.

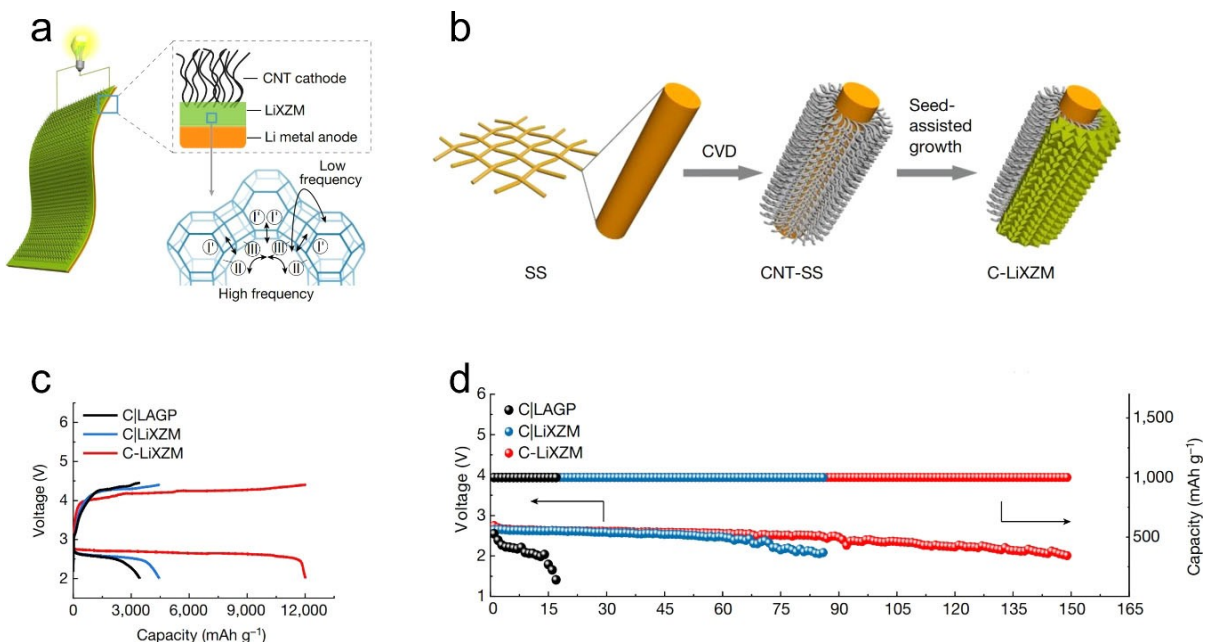


Figure 11. a) Schematic of the integrated SSLAB with C-LiXZM and the conduction mechanism of Li ions in LiX. b) Schematic of the design and preparation of the integrated C-LiXZM. CNTs were grown *in situ* on stainless-steel mesh using a chemical vapour deposition (CVD) method under a nitrogen atmosphere. After plasma treatment on one side, the zeolite membrane was grown *in situ* on the hydrophilic side of CNT-SS using a seed-assisted method. c) Specific capacities of SSLABs with integrated C-LiXZM, non-integrated C|LiXZM and C|LAGP at a current density of 500 mA g^{-1} . d) Voltage on the discharge terminal of SSLABs plotted against cycle number, at a current density of 500 mA g^{-1} and with a specific capacity limited to $1,000 \text{ mAh g}^{-1}$. Reproduced with permission from Ref. [22]. Copyright (2021) Springer Nature.

battery operation. The Gibbs free energy of each pre-assumed reaction pathway during the ORR/OER processes for the CNT@LLZTO cathode and pure CNT cathode could also be obtained through DFT calculations. This information is helpful for comparing the battery performance between the CNT@LLZTO cathode and the pure CNT cathode. Furthermore, DFT calculations also provide insights into the optimized structure and adsorption energy of Li_2O_2 on both pure CNT and LLZTO cathode surfaces. The results demonstrate that Li_2O_2 exhibits a stronger adsorption energy on the LLZTO cathode surface compared to the pure CNT surface. This suggests a more stable and secure adsorption of Li_2O_2 on the composite cathode containing LLZTO, which in turn enhances the electrochemical performance of the battery. From another perspective, *in situ* preparation of solid electrolytes on the surface of carbon-based air cathodes is also an effective way to reduce battery impedance and provide abundant triple-phase boundaries. For example, Wang et al.^[21] proposed an adjustable-porosity plastic crystal electrolyte exhibiting high ionic conductivity, excellent softness and adhesion for the first time *via* a simple controllable technique of thermally induced phase separation. The all-solid-state $\text{Li}-\text{O}_2$ battery employing this electrolyte exhibits ultra-low resistance, large capacity, good rate capability, and long cycle life.

4. Cathode Design for Solid-State Li-Air Batteries

4.1. Cathode construction for solid-state Li-air batteries

Unlike lithium-ion batteries, the air cathode material itself is not the active material for the electrode reaction during the operation of Li-air batteries, but serves to provide the site for the real electrode reactions and to store the reaction products. The total reaction in a Li-air battery is a “triple-phase” reaction involving ions (Li^+), electrons (e^-), and gas (O_2). This requires the air cathode to have good ionic and electronic conductivity, which quickly facilitate the conduction of electrons and ions to the “three-phase” interface of the $\text{Li}-\text{O}_2$ reaction. In addition, the air cathode needs to be porous because the real active material oxygen is gaseous, thus it provides good diffusivity of gas. Meanwhile, high porosity accommodates more solid discharge products Li_2O_2 , which is beneficial to increase the capacity of the battery. Moreover, since the main discharge product Li_2O_2 is an insulator, resulting in poor kinetic performance of the cell reaction, the air cathode needs to possess catalytic performance to improve the electrode reaction efficiency.

For conventional Li-air batteries with liquid organic electrolyte systems, porous carbon is the most used cathode material.^[72] Carbon materials, such as Ketjen Black, Super P, Vulcn XC-72, and carbon nanotube (CNT), are inherently good electron conductors and have a large specific surface area and catalytic sites. In addition, the liquid electrolyte has its own

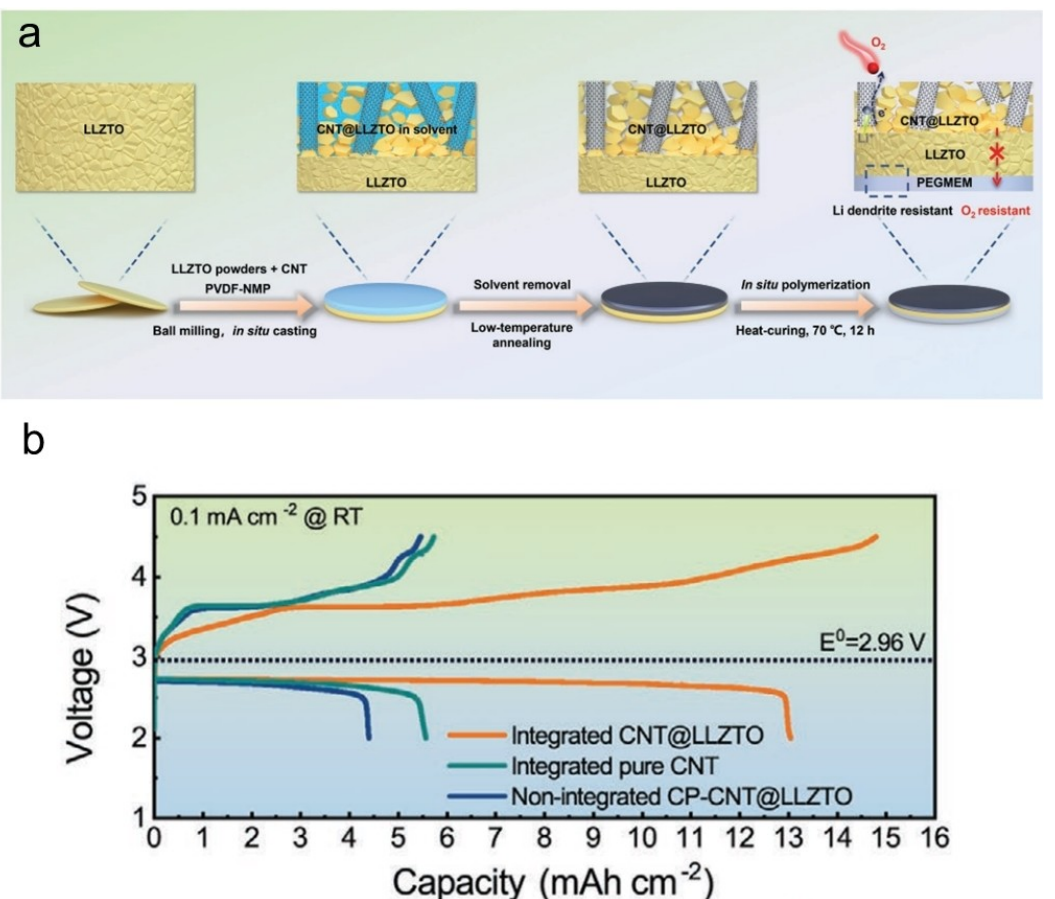


Figure 12. a) Schematic illustration of preparing integrated structure composed of LLZTO electrolyte with CNT@LLZTO cathode and PEGMEM buffer layer. b) Initial discharge/charge profiles of Li–O₂ batteries with different cathodes at 0.1 mA cm^{−2} under room temperature. Reproduced with permission from Ref. [24]. Copyright (2023) Wiley-VCH.

wettability, which can form good electron and ion transfer channels inside the carbon cathode when the cathode is wettable. However, in the design of solid-state batteries, the solid electrolyte cannot wet the cathode as the liquid electrolyte. Therefore, how to construct a solid air cathode with good

electron and ionic conductivities becomes an essential issue to be solved in battery design.

Polymer electrolytes have an advantage over inorganic solid electrolytes in constructing ion channels inside the air cathode. Balaish et al.^[14] used a self-supporting CNT woven fabric as the cathode of a Li–O₂ cell, as shown in Figure 13. There is originally

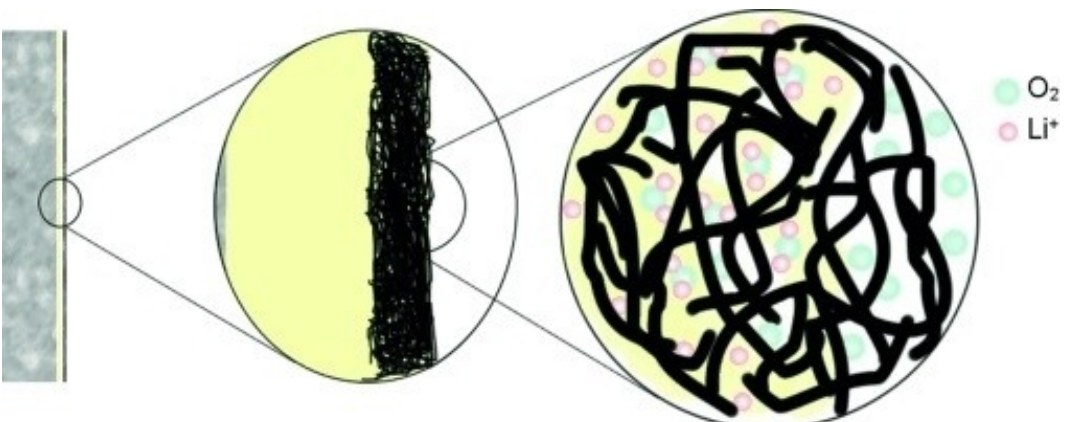


Figure 13. Schematic representation of Li–O₂ battery comprised of lithium anode (gray), P(EO)₂₀LiTf electrolyte (yellow), and CNT air-cathode (black). Reproduced with permission from Ref. [14]. Copyright (2014) Wiley-VCH.

no Li^+ transport channel inside the cathode. The cell operates at 80 °C, which is higher than the melting point of PEO, making the electrolyte soft. Bonnet-Mercier et al.^[73] reported a process similar to "hot pressing" of the cathode. The self-supported CNT film and PEO film were hot-pressed at 100 °C and 20 MPa for 10 min, and the electronic resistance of the composite anode obtained after pressure cooling was only about 1.6 Ω cm, which is comparable to that of pure CNT, indicating that the composite cathode prepared by this method has good electronic conductivity.

Due to the high melting point and hardness of the inorganic solid electrolyte, the air cathode cannot be constructed using the above high-temperature and high-pressure treatment methods. Therefore, it is a theoretically feasible solution to prepare composite air cathodes by porous carbon materials, such as Ketjen Black, Super P, and CNT, mixed with inorganic electrolyte powders by high-temperature sintering, following the idea of co-sintering electrodes for solid-state Li-air batteries. Under ideal conditions, inorganic electrolyte powders are sintered at high temperatures to form interconnected skeletons between the particles, thus providing Li^+ ion transport channels. The porous carbon material, thanks to its good electrical conductivity and high porosity, can be used as an electron transport channel and provide active sites for electrode reactions. Kumar et al.^[8] and Zhou et al.^[12,13,69a] employed ball-mill mixing, coating, and co-sintering methods to construct integrated solid-state air cathodes. These cathodes consisted of porous carbon material mixed with glass-ceramic powder, co-sintered at high temperatures. Such composite cathodes have good high temperature characteristics and can be cycled in the temperature range of 30–105 °C. Zhou et al. utilized LAGP as the solid-state electrolyte and CNT as the electron conductive agent. The composite cathode was obtained by mixing LAGP powder and CNT in different ratios, followed by sintering at 700 °C for 10 minutes under Ar atmosphere, resulting in a 50 μm thick composite cathode. The optimal performance was achieved at a LAGP to CNT weight ratio of 100:5. In another report by Kitaura et al.,^[12] a solid-state Li-air battery based on LATP electrolyte was constructed similarly by applying co-sintering method. The use of this method can reduce the

interfacial resistance between ceramic powders inside the cathode to some extent and improve the cell performance.

The type of carbon material in the air cathode also affects the performance of solid-state Li-air batteries. Liu et al.^[13] constructed solid-state air cathodes using multi-walled carbon nanotubes (MWCNT) and single-walled carbon nanotubes (SWCNT) in combination with LAGP, and investigated the battery performances. The results showed that the cathode constructed with SWCNT exhibited a higher discharge capacity and lower overpotential under the same test conditions, as shown in Figure 14. Kichambare et al.^[74] investigated the effect of doping-modified carbon materials on the performance of air cathodes. The nitrogen-doped carbon material (N-C) exhibited better electrochemical properties than the undoped material. These performance improvements are related to the fact that SWCNT and N-C have more surface defects and can provide more reactive sites. Although carbon materials are the most common conductive agents and have been widely used in the study of Li-air batteries, their side reactions with products together with strong oxidation properties during battery operation can affect the battery cycling performance. It is important to use more stable non-carbon electrodes to improve this situation. Suzuki et al.^[75] used magnetron sputtering technique to grow striated Pt electrodes on the surface of LATP solid electrolyte, and constructed a cell that can reach a discharge capacity of 300 μAh at 60 °C in oxygen.

The use of thin-film carbon material as an electron conductor within the cathode is a new idea in the design of solid-state Li-air battery cathodes. The use of thin-film systems provides better O_2 transport performance with more triple-phase boundaries. In 2011, Wang et al.^[76] presented a thin-film solid-state air cathode, where a carbon pencil-trace was used as the active electrode, "drawn" onto the surface of the LISICON solid electrolyte. TEM and Raman spectroscopy characterization show that the "drawn" cathode has a multilayer graphene structure. Zhu et al.^[18,70] reported a series of work on the design of integrated solid electrolyte-air cathode structures using template and spin-coating methods.

The Li-air battery discharge process is an oxygen reduction reaction (ORR) on the air cathode, where O_2 is reduced to the

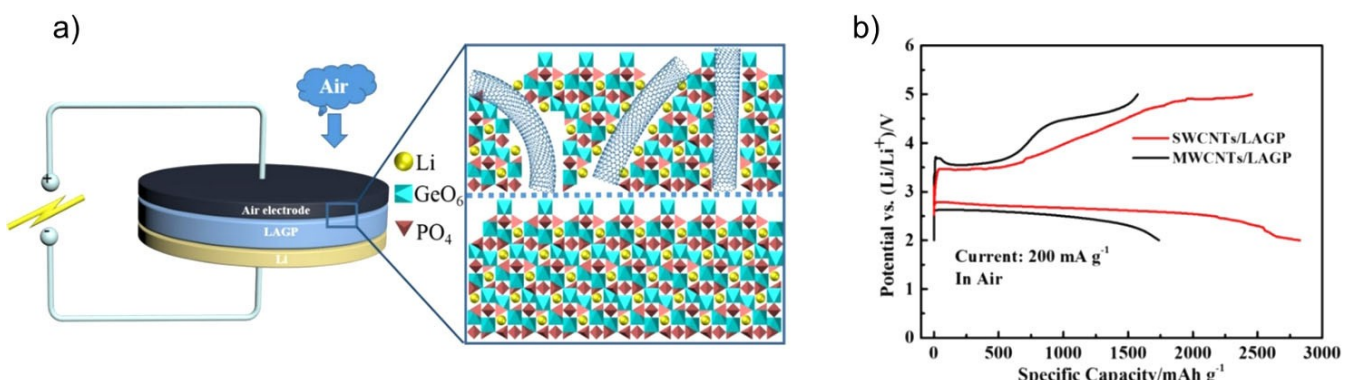


Figure 14. a) Schematic representation of the all-solid-state Li-Air battery using Li Anode, LAGP ceramic electrolyte, and an air electrode composed of SWCNTs and LAGP particles. b) First discharge-charge curves of all-solid-state Li-air batteries with SWCNTs/LAGP and MWCNTs/LAGP as air electrodes at a current density of 200 mA g⁻¹ according to weight of SWCNTs or MWCNTs. Reproduced with permission from Ref. [13]. Copyright 2015, American Chemical Society.

discharge product Li_2O_2 , while the charging process is an oxygen evolution reaction (OER) in which Li_2O_2 as a discharge product is oxidized to release O_2 on the air cathode. In the absence of catalyst, the kinetic process of discharge and charging reactions is slow and the reaction potential is high. At the same time, the insulating Li_2O_2 also leads to blocked electron transport and increased cell polarization, which affects the rate performance of the cell, accelerates the decomposition of electrolyte and air cathode material, and eventually leads to cell failure. To improve the catalytic activity of the cathode material and enhance the performance of the battery, Kitaura et al.^[12,69a,77] employed CNTs with excellent electronic conductivity and high surface area to fabricate an air cathode, combining multi-walled carbon nanotubes (MWCNTs) with ceramic electrolyte LAGP powder and co-heating them with a solid electrolyte. The air electrode contains a good electron conduction path, a continuous lithium-ion migration path and a 3D structure suitable for gas diffusion. Moreover, Li-air batteries can also utilize carbon-free cathode catalysts to promote the ORR and OER processes to facilitate the reaction kinetics on the one hand, and to improve the discharge platform, lower the charging platform, and reduce the cell polarization on the other. Currently, researchers have taken the catalysts used in fuel cells and Zn-air cells and used them in Li-air cells to improve their ORR and OER kinetic processes.

For solid-state Li-air batteries, the use of solid-phase catalysts is preferred over liquid catalysts. Solid-phase catalysts are loaded in solid form on the air cathode material of Li-air batteries. Currently, widely studied solid-phase catalysts include noble metals such as Pt,^[78] Pd,^[79] Au,^[78d,80] and Ru,^[81] and several

alloy forms or oxides of these noble metals. Transition metal oxides such as MnO_x ^[82] and Co_3O_4 ^[83] are also among the options for solid-phase catalysts in Li-air batteries. Noble metal catalysts are the first type of catalysts studied in Li-air batteries. Li-air batteries using these catalysts not only have better electrochemical performance, but also improve the discharge specific capacity and have a modulating effect on the discharge product morphology. Shen et al. designed a solid-state Li-air battery based on Pd-CNT catalytic cathode by CVD and electrochemical deposition, as shown in Figure 15.^[79b] The Pd-modified CNT cathode can effectively promote the ORR process on the cathode surface. Ru, RuO_2 as well as NiO catalysts were also shown to be effective in reducing the overpotential of OER and ORR, thereby inhibiting the by-product Li_2CO_3 generation and significantly improving the energy conversion efficiency and cyclic performance of the battery.^[5a,11b,15,72c,84] Notably, it is essential to appropriately mix carbon-free catalyst materials with solid electrolytes. This integration facilitates efficient contact for electron and Li ion pathways while maintaining a porous structure that enhances the gas diffusion and active reaction sites.

4.2. Cathode reaction mechanism in solid-state Li-air batteries

The study of the types of discharge products and the evolution of the products during the operation of the batteries are of a great significance for the study of SSLABs. Compared with Li-air batteries in liquid organic electrolyte system, the major advantage of SSLABs with respect to the study of reaction

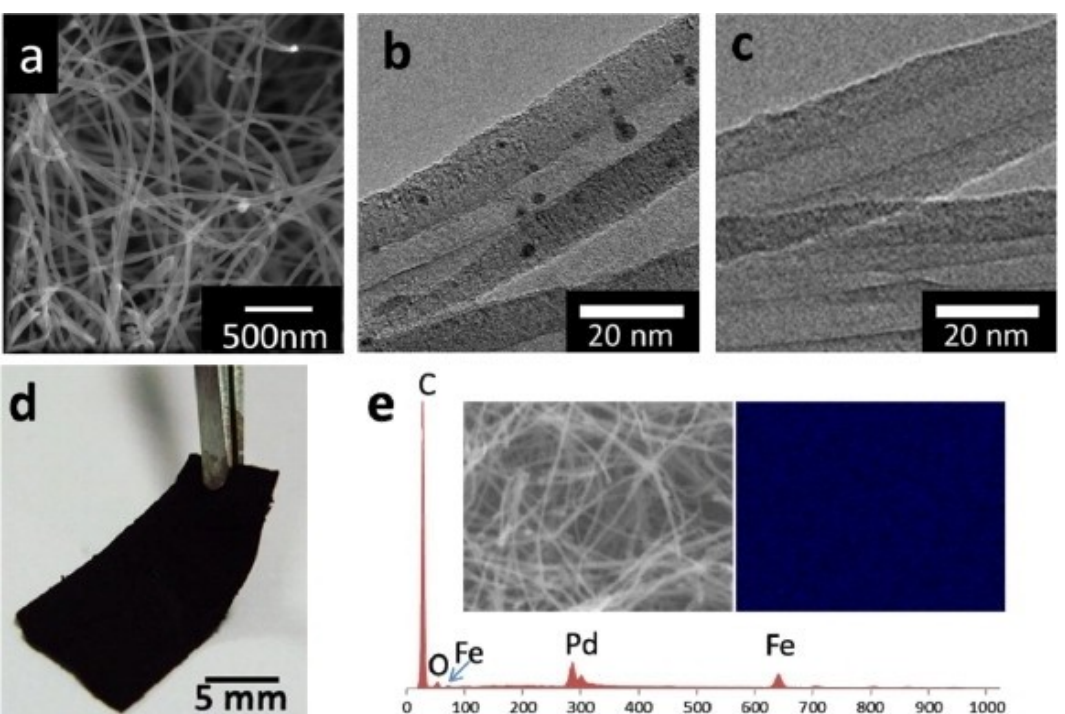


Figure 15. a) SEM image and b, c) TEM images of b) the Pd-CNT sponge and c) the pure CNT sponge. d) Optical photo of a piece of Pd-CNT sponge. e) EDX of the Pd-CNT sponge and the corresponding SEM image and Pd elemental mapping image. Reproduced with permission from Ref. [79b]. Copyright (2013) Elsevier.

mechanism is that the most unstable organic electrolyte in the current system is excluded, and thus the information about the relative truly intrinsic electrode reaction can be obtained.

Hassoun et al.^[36] studied the reaction process within the cathode under O₂ atmosphere using PEO-based solid-state Li-air batteries, as shown in Figure 16. In the PCGA analysis (potentiodynamic cycling with galvanostatic acceleration, Figure 16b), the three reduction peaks appearing during discharge correspond to the formation of LiO₂, Li₂O₂, or Li₂O, respectively, similar to those in liquid batteries. The charging process likewise displays three oxidation peaks. In addition, they propose a mechanism for Li₂O₂ oxidation (Figure 16c), like the oxidation of H₂O₂. Since the O₂^{*} to O₂ transition does not occur, the voltage observed during the actual charging process is the result of a mixture of the two processes and depends on the time of stable presence of O₂^{*} in PEO.

Zheng et al.^[85] studied the growth and decomposition process of Li₂O₂ in solid air cathode using in situ environmental SEM technique, as shown in Figure 17. SWCNT was used as the cathode, lithium metal as the anode, and the Li₂O layer on the surface of lithium metal as the solid electrolyte. When the cell is discharged, it can be observed that Li₂O₂ starts to grow at the triple-phase interface of CNT-SSE-O₂. During charging, the Li₂O₂ decomposition starts at the surface of the particles rather than

from the triple-phase interface and extends along a certain direction toward the interior of the particles (Figure 17b). This indicates that the electronic and ionic conductivity of Li₂O₂ itself can support its own decomposition under the experimental conditions. Also, they found that CNTs are covered with certain products on the surface during battery discharge and decompose during charging, which eventually leads to CNT fracture. Therefore, special attention needs to be given to the stability of carbon materials in the process of designing solid air batteries.

With the advantage that solid-state Li-air batteries can operate under atmospheric conditions, they can be used to study the mechanism of battery operation under atmospheric conditions. Kitaura et al.^[77a] studied the reaction mechanism of solid-state Li-air batteries when operating under air conditions using a LAGP/CNT composite air cathode, and the results are shown in Figure 18. When the cell is discharged, the products are firstly formed on the LAGP/CNT surface and then subjected to the action of H₂O and CO₂ in the air, which are chemically transformed into Li₂CO₃ and wrapped around the Li₂O₂ surface. The length of discharge time affects the amount of Li₂O₂ conversion. During charging, two plateaus in the curve appear, which are analyzed to correspond to Li₂O₂ and Li₂CO₃, respectively. Moreover, the high decomposition potential of Li₂CO₃ resulted in the inability of the discharge products to

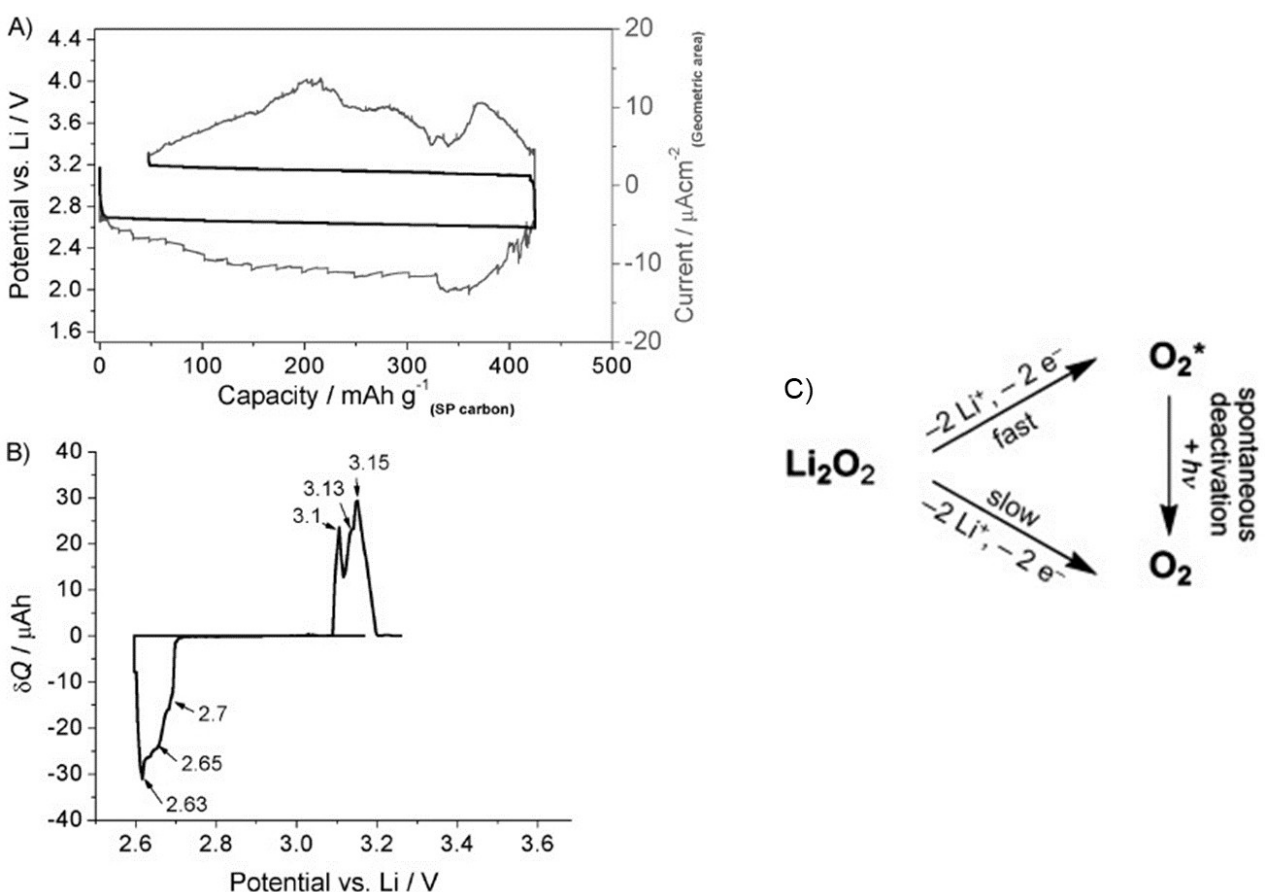


Figure 16. A) Potential (left) and current (right) versus the charge capacity normalized by the mass of the carbon and B) incremental charge (δQ) versus potential profiles of the potentiodynamic cycling with galvanostatic acceleration (PCGA) analysis performed on the cell with the configuration Li/PCE/SP-carbon, O₂. C) Proposed mechanism of lithium peroxide oxidation. Reproduced with permission from Ref. [36]. Copyright (2011) Wiley-VCH.

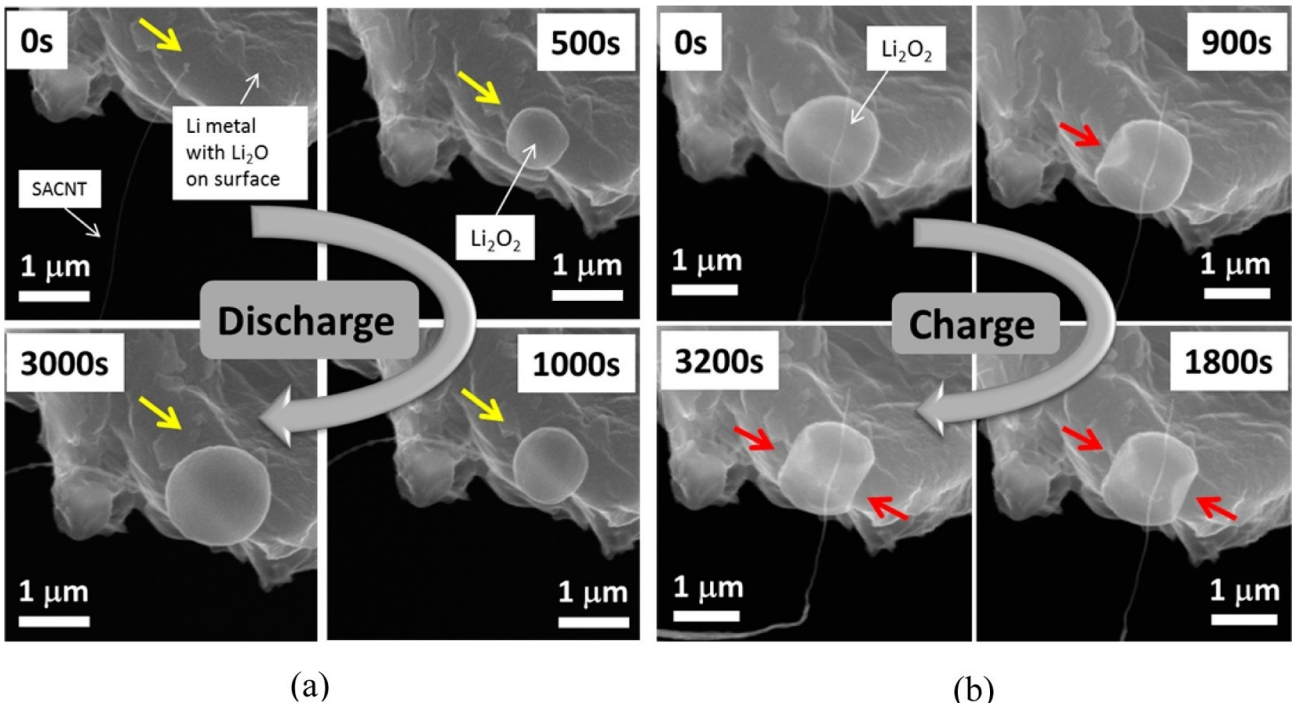


Figure 17. a) Discharge and b) charge processes of the solid-state Li–O₂ battery observed by in situ environmental SEM. Reproduced with permission from Ref. [85]. Copyright (2014) American Chemical Society.

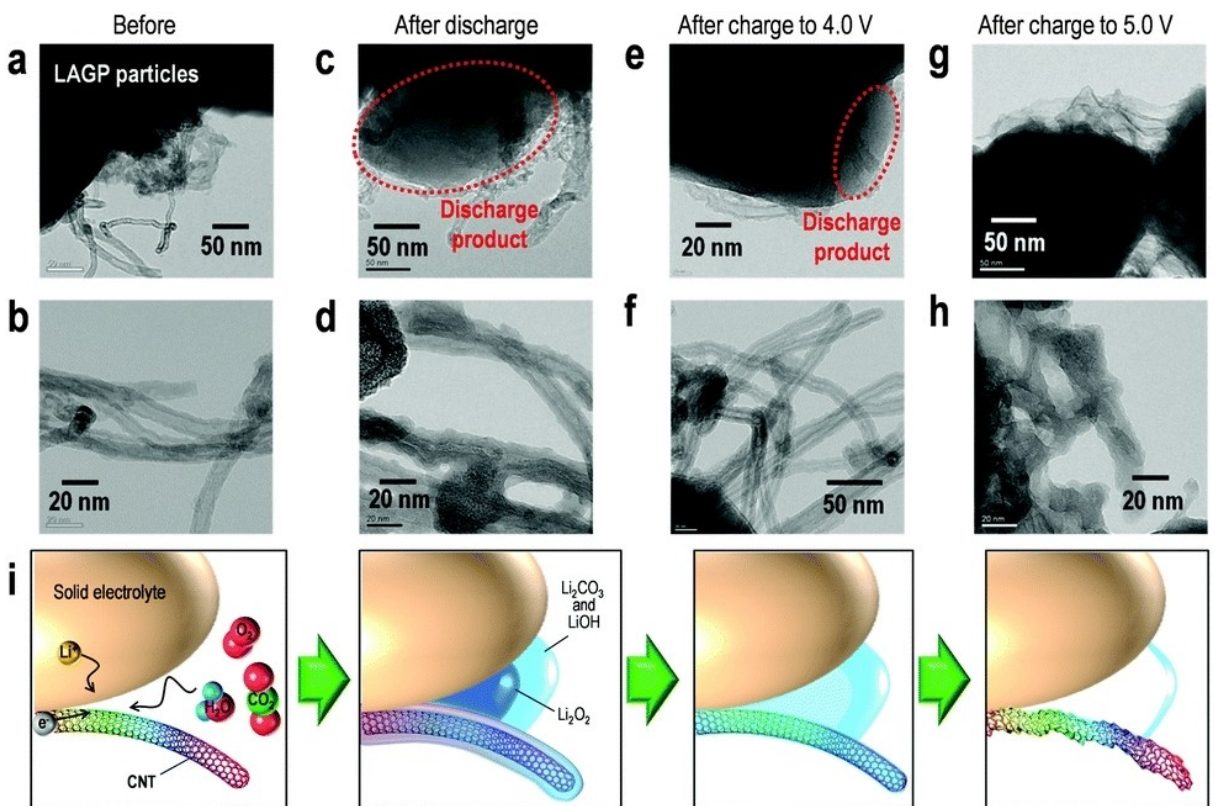


Figure 18. TEM images of the air electrode powders a, b) before discharge, c, d) after discharge, e, f) after charge to 4.0 V, and g, h) after charge to 5.0 V. i) Proposed mechanism of the all-solid-state Li-air batteries. Reproduced with permission from Ref. [77a]. Copyright (2015) Royal Society of Chemistry.

decompose completely during charging (5 V). The effect of H_2O ^[86] or CO_2 ^[87] on the products of Li-air batteries has also been studied in some literature. It is found that when the battery is operated in air, Li_2CO_3 products inevitably generate in the cathode, leading to an increase in the overcharge potential. Understanding the decomposition mechanism of Li_2CO_3 and finding catalysts that can promote its decomposition are necessary steps for the advancement of $\text{Li}-\text{O}_2$ to Li-air batteries.

5. Conclusion and Perspectives

Combining the strengths of solid-state batteries and Li-air battery systems can effectively address issues related to safety, capacity, environments, and practicality of conventional liquid lithium batteries. First, as the cornerstone of solid-state Li-air batteries, the solid electrolyte needs to meet the requirements of high ionic conductivity, good interfacial wettability, wide electrochemical window, and stability to air. It could be concluded that the use of solid electrolytes including pure electrolytes and composite electrolytes is an effective electrolyte modification strategy as they can promote electrolyte/electrode interfacial contact and maintain high conductivity simultaneously, thereby reducing the interfacial impedance inside the battery. In addition to ceramic and polymer electrolytes, there are also promising novel materials such as MOFs, COFs, and molecular sieve materials that can be utilized to develop high-performance and safe solid-state Li-air batteries. These materials offer new avenues for the evolution of this system. Second, one major challenge in the practical application of solid-state Li-air batteries is interfacial issues at the anode/electrolyte, cathode/electrolyte, and catalyst/cathode material interfaces. To address this, coating a buffer layer between the lithium anode and the electrolyte can effectively suppress lithium dendrites and enhance the interfacial stability of the electrolyte and lithium metal. The use of an alloy anode or heat treatment of lithium metal can also promote interfacial contact between lithium and electrolyte, thereby reducing battery impedance. Furthermore, reducing the electronic conductivity of the electrolyte itself can also minimize the formation of lithium dendrites. Quasi-solid Li-air batteries can be considered as a compromise instead of all-solid Li-air batteries to address the interfacial issues. Third, the cathode design of Li-air batteries still needs to be optimized, and strategies such as constructing the integrated cathode structure and the addition of catalysts can be employed to further enhance the electrochemical performance and mitigate interface resistance of solid-state Li-air batteries. Similarly, the utilization of surface-processed electrolytes and the incorporation of a dense electrolyte layer integrated with a cathode containing a porous electrolyte show promising potential for the practical implementation of solid-state lithium batteries. Yet, research gaps in the reaction mechanism of OER and ORR of solid electrolyte-based air cathode need to be narrowed. This problem is largely alleviated by the emerging technique of density functional theory (DFT) or first-principle calculations. It not only offers capability in catalytic mechanism investigation, but also assists

in the screening of cathode catalyst material. Inside the solid air cathode, because they are all in solid-solid contact, the wettability between its components is poor, which is not favorable for the transport of ions, electrons and gas molecules as well as for the storage and decomposition of discharge products. The introduction of intermediate media such as ionic liquids, redox mediators and polymer matrices helps to resolve this problem. Moreover, the construction of an integrated electrolyte and air cathode structure can effectively promote the generation of triple-phase boundaries within the battery, which in turn provides reactive sites and facilitates the transport of electrons and ions, and the diffusion of oxygen, resulting in a high-performance all-solid-state Li-air battery. However, research gap in how to improve transport and diffusivity of oxygen in solid cathodes and electrolytes remains to be narrowed.

Solid-state Li-air batteries face several challenges that can be primarily classified into three key aspects: solid electrolyte, interface modification, and air cathode. To address these challenges and improve SSLAB performance, we propose the following future work. Firstly, exploration of new materials with extraordinarily high conductivity and stability as well as compositing of these electrolyte materials with different merits, play vital role in the design of high-performance solid-state electrolytes. Secondly, breakthroughs in interface modification can be achieved through structural engineering endeavors, such as adding buffer layers to eliminate interfacial side reactions and promote solid-solid contact, or creating a porous texture of solid electrolytes to improve the contact with the electrode material. Thirdly, to facilitate the design of SSLABs in the foreseeable future, it is suggested to replace existing carbon-based cathodes with non-carbon material and deploy DFT calculations in preliminary material screening for 3D network cathodes and high-efficiency catalysts. The improvement of SSLABs is a multi-objective optimization process that inevitably comes with the bumpy road. Overall, the future prospects of solid-state lithium-air batteries in the field of energy are promising, and their potential and innovation will be further explored and realized in future research and applications.

Acknowledgements

The work was supported by the National Key R&D Program of China (Grant no. 2022YFB3807700), the National Natural Science Foundation of China (Grant no. U1964205, U21A2075, 52172253, 52102326, 52250610214), Ningbo S&T Innovation 2025 Major Special Programme (Grant No. 2018B10061, 2018B10087, 2019B10044, 2021Z122), Zhejiang Provincial Key R&D Program of China (Grant No. 2022C01072), Jiangsu Provincial S&T Innovation Special Programme for carbon peak and carbon neutrality (Grant No. BE2022007) and Youth Innovation Promotion Association CAS (Y2021080).

Conflict of Interests

The authors declare no conflict of interest.

Keywords: lithium-air batteries • solid electrolytes • air cathodes • interfacial engineering • reaction mechanisms

- [1] E. L. Littauer, K. C. Tsai, *J. Electrochem. Soc.* **1980**, *127*, 521.
- [2] K. M. Abraham, Z. Jiang, *J. Electrochem. Soc.* **1996**, *143*, 1.
- [3] a) M.-K. Song, S. Park, F. M. Alamgir, J. Cho, M. Liu, *Mater. Sci. Eng. R* **2011**, *72*, 203; b) Y. Li, X. Wang, S. Dong, X. Chen, G. Cui, *Adv. Energy Mater.* **2016**, *6*; c) H. Woo, J. Kang, J. Kim, C. Kim, S. Nam, B. Park, *Electron. Mater. Lett.* **2016**, *12*, 551.
- [4] a) H.-F. Wang, Q. Xu, *Matter* **2019**, *1*, 565; b) T. Ogasawara, A. Debart, M. Holzapfel, P. Novak, P. G. Bruce, *J. Am. Chem. Soc.* **2006**, *128*, 1390; c) L. Johnson, C. M. Li, Z. Liu, Y. H. Chen, S. A. Freunberger, P. C. Ashok, B. B. Praveen, K. Dholakia, J. M. Tarascon, P. G. Bruce, *Nat. Chem.* **2014**, *6*, 1091; d) W. J. Kwak, J. B. Park, H. G. Jung, Y. K. Sun, *ACS Energy Lett.* **2017**, *2*, 2756.
- [5] a) M. M. O. Thotiyil, S. A. Freunberger, Z. Q. Peng, Y. H. Chen, Z. Liu, P. G. Bruce, *Nat. Mater.* **2013**, *12*, 1049; b) J. Lu, L. Li, J. B. Park, Y. K. Sun, F. Wu, K. Amine, *Chem. Rev.* **2014**, *114*, 5611; c) N. Feng, P. He, H. Zhou, *Adv. Energy Mater.* **2016**, *6*; d) X. Xin, K. Ito, Y. Kubo, *Electrochim. Acta* **2018**, *261*, 323; e) C. Z. Shu, J. Z. Wang, J. P. Long, H. K. Liu, S. X. Dou, *Adv. Mater.* **2019**, *31*, 43; f) Y. Liu, L. P. Wang, L. J. Cao, C. Q. Shang, Z. Y. Wang, H. E. Wang, L. Q. He, J. Y. Yang, H. Cheng, J. Z. Li, Z. G. Lu, *Mater. Chem. Front.* **2017**, *1*, 2495.
- [6] J. Lai, Y. Xing, N. Chen, L. Li, F. Wu, R. Chen, *Angew. Chem. Int. Ed. Engl.* **2020**, *59*, 2974.
- [7] L. L. Luo, B. Liu, S. D. Song, W. Xu, J. G. Zhang, C. M. Wang, *Nat. Nanotechnol.* **2017**, *12*, 535.
- [8] B. Kumar, J. Kumar, R. Leese, J. P. Fellner, S. J. Rodrigues, K. M. Abraham, *J. Electrochem. Soc.* **2010**, *157*, A50.
- [9] a) Z. J. Liang, W. W. Wang, Y. C. Lu, *Joule* **2022**, *6*, 2458; b) C. S. Yang, K. N. Gao, X. P. Zhang, Z. Sun, T. Zhang, *Rare Met.* **2018**, *37*, 459; c) L. Wang, J. Pan, Y. Zhang, X. Cheng, L. Liu, H. Peng, *Adv. Mater.* **2018**, *30*.
- [10] a) J. Yi, S. H. Guo, P. He, H. S. Zhou, *Energy Environ. Sci.* **2017**, *10*, 860; b) W. Zhao, X. Mu, P. He, H. Zhou, *Batteries & Supercaps* **2019**, *2*, 803; c) W. J. Song, S. Yoo, G. Song, S. Lee, M. Kong, J. Rim, U. Jeong, S. Park, *Batteries & Supercaps* **2019**, *2*, 181; d) Z. Liang, Y. C. Lu, J. Am. Chem. Soc. **2016**, *138*, 7574.
- [11] a) Z. Y. Guo, C. Li, J. Y. Liu, Y. G. Wang, Y. Y. Xia, *Angew. Chem. Int. Ed.* **2017**, *56*, 7505; b) X. B. Zhu, T. S. Zhao, P. Tan, Z. H. Wei, M. C. Wu, *Nano Energy* **2016**, *26*, 565.
- [12] H. Kitaura, H. Zhou, *Energy Environ. Sci.* **2012**, *5*, 9077.
- [13] Y. J. Liu, B. J. Li, H. Kitaura, X. P. Zhang, M. Han, P. He, H. S. Zhou, *ACS Appl. Mater. Interfaces* **2015**, *7*, 17307.
- [14] M. Balaish, E. Peled, D. Golodnitsky, Y. Ein-Eli, *Angew. Chem.* **2015**, *127*, 446.
- [15] Y. J. Liu, B. J. Li, Z. Cheng, C. Li, X. Y. Zhang, S. H. Guo, P. He, H. S. Zhou, *J. Power Sources* **2018**, *395*, 439.
- [16] Y. J. Liu, C. Li, B. J. Li, H. C. Song, Z. Cheng, M. R. Chen, P. He, H. S. Zhou, *Adv. Energy Mater.* **2018**, *8*, 7.
- [17] S. Wang, J. Wang, J. Liu, H. Song, Y. Liu, P. Wang, P. He, J. Xu, H. Zhou, *J. Mater. Chem. A* **2018**, *6*, 21248.
- [18] X. B. Zhu, T. S. Zhao, Z. H. Wei, P. Tan, L. An, *Energy Environ. Sci.* **2015**, *8*, 3745.
- [19] C. Zhao, Q. Sun, J. Luo, J. Liang, Y. Liu, L. Zhang, J. Wang, S. Deng, X. Lin, X. Yang, H. Huang, S. Zhao, L. Zhang, S. Lu, X. Sun, *Chem. Mater.* **2020**, *32*, 10113.
- [20] W. Yu, C. Xue, B. Hu, B. Xu, L. Li, C.-W. Nan, *Energy Storage Mater.* **2020**, *27*, 244.
- [21] J. Wang, G. Huang, K. Chen, X. B. Zhang, *Angew. Chem. Int. Ed.* **2020**, *59*, 9382.
- [22] X. Chi, M. Li, J. Di, P. Bai, L. Song, X. Wang, F. Li, S. Liang, J. Xu, J. Yu, *Nature* **2021**, *592*, 551.
- [23] H. Liu, L. Zhao, Y. Xing, J. Lai, L. Li, F. Wu, N. Chen, R. Chen, *ACS Appl. Energ. Mater.* **2022**, *5*, 7185.
- [24] Z. Gu, X. Xin, Z. Xu, J. He, J. Wu, Y. Sun, X. Yao, *Adv. Funct. Mater.* **2023**, DOI: 10.1002/adfm.202301583.
- [25] A. Kondori, M. Esmaeilirad, A. M. Harzandi, R. Amine, M. T. Saray, L. Yu, T. Liu, J. Wen, N. Shan, H.-H. Wang, A. T. Ngo, P. C. Redfern, C. S. Johnson, K. Amine, R. Shahbazian-Yassar, L. A. Curtiss, M. Asadi, *Science* **2023**, *379*, 499.
- [26] D. E. Fenton, J. M. Parker, P. V. Wright, *Polymer* **1973**, *14*, 589.
- [27] a) Y. Zhang, L. Wang, Z. Y. Guo, Y. F. Xu, Y. G. Wang, H. S. Peng, *Angew. Chem. Int. Ed.* **2016**, *55*, 4487; b) L. Wang, Y. Zhang, J. Pan, H. S. Peng, *J. Mater. Chem. A* **2016**, *4*, 13419.
- [28] a) Q. C. Liu, T. Liu, D. P. Liu, Z. J. Li, X. B. Zhang, Y. Zhang, *Adv. Mater.* **2016**, *28*, 8413; b) T. Liu, Q. C. Liu, J. J. Xu, X. B. Zhang, *Small* **2016**, *12*, 3101.
- [29] C. W. Sun, J. Liu, Y. D. Gong, D. P. Wilkinson, J. J. Zhang, *Nano Energy* **2017**, *33*, 363.
- [30] a) H. Kim, T. Y. Kim, V. Roev, H. C. Lee, H. J. Kwon, H. Lee, S. Kwon, D. Im, *ACS Appl. Mater. Interfaces* **2016**, *8*, 1344; b) M. Balaish, E. Peled, D. Golodnitsky, Y. Ein-Eli, *Angew. Chem. Int. Ed.* **2015**, *54*, 436; c) K. N. Jung, J. I. Lee, J. H. Jung, K. H. Shin, J. W. Lee, *Chem. Commun.* **2014**, *50*, 5458; d) J. Yi, X. Z. Liu, S. H. Guo, K. Zhu, H. L. Xue, H. S. Zhou, *ACS Appl. Mater. Interfaces* **2015**, *7*, 23798.
- [31] E. Quararone, P. Mustarelli, *Chem. Soc. Rev.* **2011**, *40*, 2525.
- [32] J. W. Fergus, *J. Power Sources* **2010**, *195*, 4554.
- [33] E. Tsuchida, H. Ohno, K. Tsunemi, N. Kobayashi, *Solid State Ionics* **1983**, *11*, 227.
- [34] E. Quararone, P. Mustarelli, A. Magistris, *Solid State Ionics* **1998**, *110*, 1.
- [35] a) C. H. Wang, Y. F. Yang, X. J. Liu, H. Zhong, H. Xu, Z. B. Xu, H. X. Shao, F. Ding, *ACS Appl. Mater. Interfaces* **2017**, *9*, 13694; b) J. H. Choi, C. H. Lee, J. H. Yu, C. H. Doh, S. M. Lee, *J. Power Sources* **2015**, *274*, 458; c) J. Zheng, M. X. Tang, Y. Y. Hu, *Angew. Chem. Int. Ed.* **2016**, *55*, 12538; d) K. M. Nairn, A. S. Best, P. J. Newman, D. R. MacFarlane, M. Forsyth, *Solid State Ionics* **1999**, *121*, 115.
- [36] J. Hassoun, F. Croce, M. Armand, B. Scrosati, *Angew. Chem. Int. Ed.* **2011**, *50*, 2999.
- [37] P. Birke, F. Salam, S. Doring, W. Weppner, *Solid State Ionics* **1999**, *118*, 149.
- [38] G. Y. Adachi, N. Imanaka, H. Aono, *Adv. Mater.* **1996**, *8*, 127.
- [39] S. Stramare, V. Thangadurai, W. Weppner, *Chem. Mater.* **2003**, *15*, 3974.
- [40] a) Y. Zhao, L. L. Daemen, *J. Am. Chem. Soc.* **2012**, *134*, 15042; b) S. Li, J. Zhu, Y. Wang, J. W. Howard, X. Lu, Y. Li, R. S. Kumar, L. Wang, L. L. Daemen, Y. Zhao, *Solid State Ionics* **2016**, *284*, 14; c) Z. D. Hood, H. Wang, A. S. Pandian, J. K. Keum, C. Liang, *J. Am. Chem. Soc.* **2016**, *138*, 1768; d) A. Emly, E. Kioupakis, A. Van der Ven, *Chem. Mater.* **2013**, *25*, 4663.
- [41] J. B. Goodenough, H. Y. P. Hong, J. A. Kafalas, *Mater. Res. Bull.* **1976**, *11*, 203.
- [42] Y. P. Hong, *Mater. Res. Bull.* **1976**, *11*, 173.
- [43] W. Hou, X. Guo, X. Shen, K. Amine, H. Yu, J. Lu, *Nano Energy* **2018**, *52*, 279.
- [44] a) Z. Jian, Y.-S. Hu, X. Ji, W. Chen, *Adv. Mater.* **2017**, *29*, 1601925; b) D. Mazza, *J. Solid State Chem.* **2001**, *156*, 154.
- [45] a) H. Kohler, H. Schulz, O. Melnikov, *Mater. Res. Bull.* **1983**, *18*, 1143; b) U. V. Alpen, M. F. Bell, W. Wichelhaus, *Mater. Res. Bull.* **1979**, *14*, 1317.
- [46] H. Aono, E. Sugimoto, Y. Sadaoka, N. Imanaka, G. Y. Adachi, *J. Electrochem. Soc.* **1989**, *136*, 590.
- [47] H. Aono, E. Sugimoto, Y. Sadaoka, N. Imanaka, G. Y. Adachi, *Bull. Chem. Soc. Jpn.* **1992**, *65*, 2200.
- [48] V. Thangadurai, H. Kaack, W. J. F. Weppner, *J. Am. Ceram. Soc.* **2003**, *86*, 437.
- [49] R. Murugan, V. Thangadurai, W. Weppner, *Angew. Chem. Int. Ed.* **2007**, *46*, 7778.
- [50] J. Awaka, N. Kijima, H. Hayakawa, J. Akimoto, *J. Solid State Chem.* **2009**, *182*, 2046.
- [51] J. Awaka, A. Takashima, K. Kataoka, N. Kijima, Y. Idemoto, J. Akimoto, *Chem. Lett.* **2011**, *40*, 60.
- [52] C. Wang, K. Fu, S. P. Kammampata, D. W. McOwen, A. J. Samson, L. Zhang, G. T. Hitz, A. M. Nolan, E. D. Wachsman, Y. Mo, V. Thangadurai, L. Hu, *Chem. Rev.* **2020**, *120*, 4257.
- [53] J. Y. Sun, N. Zhao, Y. Q. Li, X. X. Guo, X. F. Feng, X. S. Liu, Z. Liu, G. L. Cui, H. Zheng, L. Gu, H. Li, *Sci. Rep.* **2017**, *7*, 8.
- [54] a) Y. Kato, S. Hori, T. Saito, K. Suzuki, M. Hirayama, A. Mitsui, B. Yonemura, H. Iba, R. Kanno, *Nat. Energy* **2016**, *1*; b) Z. Zhang, Y. Shao, B. Lotsch, Y.-S. Hu, H. Li, J. Janek, L. F. Nazar, C.-W. Nan, J. Maier, M. Armand, L. Chen, *Energy Environ. Sci.* **2018**, *11*, 1945.
- [55] a) K. H. Nie, Y. S. Hong, J. L. Qiu, Q. H. Li, X. Q. Yu, H. Li, L. Q. Chen, *Front. Chem.* **2018**, *6*; b) J.-M. Doux, Y. Yang, D. H. S. Tan, N. Han, E. A. Wu, X. Wang, A. Banerjee, Y. S. Meng, *J. Mater. Chem. A* **2020**, *8*, 5049.
- [56] J. Wu, S. Liu, F. Han, X. Yao, C. Wang, *Adv. Mater.* **2021**, *33*, e2000751.

- [57] S. Chen, D. Xie, G. Liu, J. P. Mwizerwa, Q. Zhang, Y. Zhao, X. Xu, X. Yao, *Energy Storage Mater.* **2018**, *14*, 58.
- [58] a) G. Liu, D. Xie, X. Wang, X. Yao, S. Chen, R. Xiao, H. Li, X. Xu, *Energy Storage Mater.* **2019**, *17*, 266; b) H. Wang, Y. Chen, Z. D. Hood, G. Sahu, A. S. Pandian, J. K. Keum, K. An, C. Liang, *Angew. Chem. Int. Ed.* **2016**, *55*, 8551.
- [59] K. Noriaki, H. Kenji, Y. Yuichiro, H. Masaaki, K. Ryoji, Y. Masao, K. Takashi, K. Yuki, H. Shigenori, K. Koji, *Nat. Mater.* **2011**, *10*, 682.
- [60] X. X. Wang, D. H. Guan, C. L. Miao, D. C. Kong, L. J. Zheng, J. J. Xu, *J. Am. Chem. Soc.* **2023**, *145*, 5718.
- [61] X.-X. Wang, X.-W. Chi, M.-L. Li, D.-H. Guan, C.-L. Miao, J.-J. Xu, *Chem* **2023**, *9*, 394.
- [62] a) F. Agusse, W. Manalastas, L. Buannic, J. M. L. del Amo, G. Singh, A. Llordes, J. Kilner, *ACS Appl. Mater. Interfaces* **2017**, *9*, 3808; b) R. Zhang, X. Shen, X. B. Cheng, Q. Zhang, *Energy Storage Mater.* **2019**, *23*, 556.
- [63] A. Sharifi, H. M. Meyer, J. Nanda, J. Wolfenstein, J. Sakamoto, *J. Power Sources* **2016**, *302*, 135.
- [64] a) W. Luo, Y. H. Gong, Y. Z. Zhu, K. K. Fu, J. Q. Dai, S. D. Lacey, C. W. Wang, B. Y. Liu, X. G. Han, Y. F. Mo, E. D. Wachsman, L. B. Hu, *J. Am. Chem. Soc.* **2016**, *138*, 12258; b) W. Luo, Y. H. Gong, Y. Z. Zhu, Y. J. Li, Y. G. Yao, Y. Zhang, K. Fu, G. Pastel, C. F. Lin, Y. F. Mo, E. D. Wachsman, L. B. Hu, *Adv. Mater.* **2017**, *29*, 7; c) C. W. Wang, Y. H. Gong, B. Y. Liu, K. Fu, Y. G. Yao, E. Hitz, Y. J. Li, J. Q. Dai, S. M. Xu, W. Luo, E. D. Wachsman, L. B. Hu, *Nano Lett.* **2017**, *17*, 565; d) X. G. Han, Y. H. Gong, K. Fu, X. F. He, G. T. Hitz, J. Q. Dai, A. Pearse, B. Y. Liu, H. Wang, G. Rublo, Y. F. Mo, V. Thangadurai, E. D. Wachsman, L. B. Hu, *Nat. Mater.* **2017**, *16*, 572; e) K. Hofstetter, A. J. Samson, S. Narayanan, V. Thangadurai, *J. Power Sources* **2018**, *390*, 297.
- [65] C. L. Tsai, V. Roddatis, C. V. Chandran, Q. L. Ma, S. Uhlenbruck, M. Bram, P. Heijmans, O. Guillou, *ACS Appl. Mater. Interfaces* **2016**, *8*, 10617.
- [66] Z. Gu, X. Xin, J. Yang, D. C. Guo, S. J. Yang, J. H. Wu, Y. Sun, X. Y. Yao, *ACS Appl. Energ. Mater.* **2022**, *5*, 9149.
- [67] Y. J. Shao, H. C. Wang, Z. L. Gong, D. W. Wang, B. Z. Zheng, J. P. Zhu, Y. X. Lu, Y. S. Hu, X. X. Guo, H. Li, X. J. Huang, Y. Yang, C. W. Nan, L. Q. Chen, *ACS Energy Lett.* **2018**, *3*, 1212.
- [68] L. Zhong, R. R. Mitchell, Y. Liu, B. M. Gallant, C. V. Thompson, J. Y. Huang, S. X. Mao, Y. Shao-Horn, *Nano Lett.* **2013**, *13*, 2209.
- [69] a) H. Kitaura, H. S. Zhou, *Adv. Energy Mater.* **2012**, *2*, 889; b) H. Kitaura, H. S. Zhou, *Energy Environ. Sci.* **2012**, *5*, 9077.
- [70] X. B. Zhu, T. S. Zhao, Z. H. Wei, P. Tan, G. Zhao, *Energy Environ. Sci.* **2015**, *8*, 2782.
- [71] C. Li, Y. J. Liu, B. J. Li, F. Zhang, Z. Cheng, P. He, H. S. Zhou, *Nanotechnology* **2019**, *30*, 7.
- [72] a) Y. Lei, J. Lu, X. Y. Luo, T. P. Wu, P. Du, X. Y. Zhang, Y. Ren, J. G. Wen, D. J. Miller, J. T. Miller, Y. K. Sun, J. W. Elam, K. Amine, *Nano Lett.* **2013**, *13*, 4182; b) J. G. Zhang, D. Y. Wang, W. Xu, J. Xiao, R. E. Williford, J. Power Sources **2010**, *195*, 4332; c) Z. Q. Peng, S. A. Freunberger, Y. H. Chen, P. G. Bruce, *Science* **2012**, *337*, 563; d) Y. C. Lu, H. A. Gasteiger, Y. Shao-Horn, *Electrochem. Solid-State Lett.* **2011**, *14*, A70; e) Y. F. Li, Z. P. Huang, K. Huang, D. Carnahan, Y. C. Xing, *Energy Environ. Sci.* **2013**, *6*, 3339; f) T. H. Yoon, Y. J. Park, *Nanoscale Res. Lett.* **2012**, *7*, 1; g) D. A. Agyeman, M. Park, Y. M. Kang, *J. Mater. Chem. A* **2017**, *5*, 22234.
- [73] N. Bonnet-Mercier, R. A. Wong, M. L. Thomas, A. Dutta, K. Yamanaka, C. Yogi, T. Ohta, H. R. Byon, *Sci. Rep.* **2014**, *4*, 7.
- [74] P. Kichambare, J. Kumar, S. Rodrigues, B. Kumar, *J. Power Sources* **2011**, *196*, 3310.
- [75] a) Y. Suzuki, K. Watanabe, S. Sakuma, N. Imanishi, *Solid State Ionics* **2016**, *289*, 72; b) Y. Suzuki, K. Kami, K. Watanabe, N. Imanishi, *Solid State Ionics* **2015**, *278*, 222.
- [76] Y. G. Wang, H. S. Zhou, *Energy Environ. Sci.* **2011**, *4*, 1704.
- [77] a) H. Kitaura, H. S. Zhou, *Chem. Commun.* **2015**, *51*, 17560; b) H. Kitaura, H. S. Zhou, *Sci. Rep.* **2015**, *5*, 8.
- [78] a) G. Y. Zhao, J. X. Lv, Z. M. Xu, L. Zhang, K. N. Sun, *J. Power Sources* **2014**, *248*, 1270; b) H. D. Lim, H. Song, H. Gwon, K. Y. Park, J. Kim, Y. Bae, H. Kim, S. K. Jung, T. Kim, Y. H. Kim, X. Lepro, R. Ovalle-Robles, R. H. Baughman, K. Kang, *Energy Environ. Sci.* **2013**, *6*, 3570; c) D. W. Su, H. S. Kim, W. S. Kim, G. X. Wang, *J. Power Sources* **2013**, *244*, 488; d) Y. C. Lu, Z. C. Xu, H. A. Gasteiger, S. Chen, K. Hamad-Schifferli, Y. Shao-Horn, *J. Am. Chem. Soc.* **2010**, *132*, 12170.
- [79] a) R. Choi, J. Jung, G. Kim, K. Song, Y. I. Kim, S. C. Jung, Y. K. Han, H. Song, Y. M. Kang, *Energy Environ. Sci.* **2014**, *7*, 1362; b) Y. Shen, D. Sun, L. Yu, W. Zhang, Y. Y. Shang, H. R. Tang, J. F. Wu, A. Y. Cao, Y. H. Huang, *Carbon* **2013**, *62*, 288.
- [80] a) D. W. Su, S. X. Dou, G. X. Wang, *NPG Asia Mater.* **2015**, *7*, 12; b) W. G. Fan, X. X. Guo, D. D. Xiao, L. Gu, *J. Phys. Chem. C* **2014**, *118*, 7344.
- [81] a) F. J. Li, Y. Chen, D. M. Tang, Z. L. Jian, C. Liu, D. Golberg, A. Yamada, H. S. Zhou, *Energy Environ. Sci.* **2014**, *7*, 1648; b) G. Y. Zhao, Y. N. Niu, L. Zhang, K. N. Sun, *J. Power Sources* **2014**, *270*, 386; c) Y. Yang, W. Liu, Y. M. Wang, X. C. Wang, L. Xiao, J. T. Lu, L. Zhuang, *Phys. Chem. Chem. Phys.* **2014**, *16*, 20618; d) H. G. Jung, Y. S. Jeong, J. B. Park, Y. K. Sun, B. Scrosati, Y. J. Lee, *ACS Nano* **2013**, *7*, 3532; e) K. Guo, Y. Li, J. Yang, Z. Q. Zou, X. Z. Xue, X. M. Li, H. Yang, *J. Mater. Chem. A* **2014**, *2*, 1509; f) Z. L. Jian, P. Liu, F. J. Li, P. He, X. W. Guo, M. W. Chen, H. S. Zhou, *Angew. Chem. Int. Ed.* **2014**, *53*, 442.
- [82] a) Z. H. Cui, X. X. Guo, *J. Power Sources* **2014**, *267*, 20; b) T. T. Truong, Y. Z. Liu, Y. Ren, L. Trahey, Y. G. Sun, *ACS Nano* **2012**, *6*, 8067.
- [83] a) C. W. Sun, F. Li, C. Ma, Y. Wang, Y. L. Ren, W. Yang, Z. H. Ma, J. Q. Li, Y. J. Chen, Y. Kim, L. Q. Chen, *J. Mater. Chem. A* **2014**, *2*, 7188; b) D. S. Kim, Y. J. Park, *J. Alloys Compd.* **2014**, *591*, 164.
- [84] a) F. Li, D.-M. Tang, T. Zhang, K. Liao, P. He, D. Golberg, A. Yamada, H. Zhou, *Adv. Energy Mater.* **2015**, *5*; b) K. Liao, X. Wang, Y. Sun, D. Tang, M. Han, P. He, X. Jiang, T. Zhang, H. Zhou, *Energy Environ. Sci.* **2015**, *8*, 1992; c) P. Tan, Z. H. Wei, W. Shyy, T. S. Zhao, X. B. Zhu, *Energy Environ. Sci.* **2016**, *9*, 1783.
- [85] H. Zheng, D. D. Xiao, X. Li, Y. L. Liu, Y. Wu, J. P. Wang, K. L. Jiang, C. Chen, L. Gu, X. L. Wei, Y. S. Hu, Q. Chen, H. Li, *Nano Lett.* **2014**, *14*, 4245.
- [86] X. F. Wang, S. R. Cai, D. Zhu, S. J. Mu, Y. G. Chen, *J. Solid State Electrochem.* **2015**, *19*, 2421.
- [87] a) S. R. Gowda, A. Brunet, G. M. Wallraff, B. D. McCloskey, *J. Phys. Chem. Lett.* **2013**, *4*, 276; b) H. K. Lim, H. D. Lim, K. Y. Park, D. H. Seo, H. Gwon, J. Hong, W. A. Goddard, H. Kim, K. Kang, *J. Am. Chem. Soc.* **2013**, *135*, 9733; c) Y. M. Du, Y. J. Liu, S. X. Yang, C. Li, Z. Cheng, F. L. Qiu, P. He, H. S. Zhou, *J. Mater. Chem. A* **2021**, *9*, 9581.

Manuscript received: June 25, 2023

Revised manuscript received: August 9, 2023

Accepted manuscript online: August 10, 2023

Version of record online: August 28, 2023